AALBORG UNIVERSITY

Techno-economic and environmental assessment of the coordinated operation of regional grid-connected energy hubs considering high penetration of wind power

Zare Oskouei, Morteza ; Mohammadi-Ivatloo, Behnam ; Abapour, Mehdi; Shafiee, Mahmood; Anvari-Moghaddam, Amjad

Techno-economic and environmental assessment of the coordinated operation of regional grid-connected energy hubs considering high penetration of wind power

Morteza Zare Oskouei[a], Behnam Mohammadi-Ivatloo[a,*], Mehdi Abapour[a], Mahmood Shafiee[b], Amjad Anvari-Moghaddam[a,c]

[a]*Smart Energy Systems Laboratory, Faculty of Electrical and Computer Engineering, University of Tabriz, Tabriz, Iran*
[b]*School of Engineering and Digital Arts, University of Kent, Canterbury, UK*
[c]*Department of Energy Technology, Aalborg University, 9220 Aalborg East, Denmark*

Abstract

Nowadays, the high penetration of renewable energy sources (RESs) with non-uniformly distributed patterns has created unprecedented challenges for regional power systems to maintain system flexibility and reliability. These technical challenges obligate power system operators to curtail part of the produced renewable energy at various scheduling intervals. Motivated by these challenges, grid-connected energy hubs are seen as a way forward to boost system flexibility, decrease the rate of renewable power curtailment, and increase energy efficiency. However, simplified models may significantly affect the performance of the grid-connected energy hubs in practice. Hence, this paper proposes a holistic structure to determine the optimal coordinated operation of the grid-connected energy hubs and the regional power system by relying on the high penetration of wind power. In this regard, various fundamental challenges that have not yet been addressed in an integrated manner, including the CO_2 emission rate and the amount of curtailed renewable energy along with total operating costs of the integrated energy system, are among the main objectives of the optimization problem. The proposed structure is developed in the form of tractable mixed-integer nonlinear programming (MINLP) problem to handle the day-ahead security-constrained unit commitment (SCUC). The information-gap decision theory (IGDT)-based robust model is used for accurate modeling of wind power uncertainty. The characteristics of the proposed IGDT-based robust SCUC model and its benefits are investigated through several technical case studies conducted on the modified 6-bus and 24-bus test systems. The simulation results validate the effectiveness and feasibility of the proposed structure. According to the obtained results for the 6-bus test system, networked energy hubs can help the system operator to reduce the total operating cost, wind power curtailment cost, and CO_2 emission cost by 16.62%, 100%, and 30.44%, respectively, through utilizing up-to-date energy conversion facilities and energy storage systems as well as managing energy demands. It can be seen that the proposed strategy is a very effective step towards achieving a 100% renewable energy system.

Keywords: Demand response, energy hubs, energy storage systems, information-gap decision theory (IGDT), multi-carrier energy systems, renewable power curtailment.

---

*Corresponding author
Email address:* bmohammadi@tabrizu.ac.ir (Behnam Mohammadi-Ivatloo)

Nomenclature

Acronyms

CHP	Combined heat and power.
DRP	Demand response program.
EESs	Electrical energy storages.
GB	Gas boiler.
IGDT	Information-gap decision theory.
P2H	Power-to-heat.
RESs	Renewable energy sources.
TESs	Thermal energy storages.

Indices (sets)

b (NB), i (NI), l (NL)	Indices of buses, thermal units, and transmission lines.
es (NES), ts (NTS)	Indices of electrical and thermal energy storages.
q(NQ), g (NG), ph (NPH)	Indices of CHP units, gas boilers, and P2H storages.
m (NM), n (NN), w (NW)	Indices of electrical loads, heat loads, and wind farms.
t (NT)	Index of time interval.

Parameters

I. General parameters:

$EL_{m,t}^{ini}$, $HL_{n,t}^{ini}$	Initial electrical and heat demands at hour t.
FR_t^{up}, FR_t^{dw}	System up/down flexible ramping reserves requirement at hour t.
$\overline{F_l}$	Transmission line l capacity.
IE, IH	Rate of incentive for electrical and heat demands variation.
$P_{w,t}$	Forecasted wind power output of wind farm w at hour t.
$KI_{b,i}$, $KW_{b,w}$	Bus-thermal unit, bus-wind farm incidence matrices.
$KQ_{b,q}$, $KG_{b,g}$	Bus-CHP unit, bus-gas boiler unit incidence matrices.
$KE_{b,es}$, $KT_{b,ts}$	Bus-electrical storage, bus-thermal storage incidence matrices.
$KM_{b,m}$, $KN_{b,n}$	Bus-electrical load, bus-heat load incidence matrices.
$KP_{b,ph}$, $KL_{b,l}$	Bus-P2H storage, bus-branch incidence matrices.
TC_c	Cost target for the robustness function.
TC_d	Base level of the objective function.
em_i, em_q, em_g	Carbon emissions quota of thermal, CHP, and gas boiler units.
x_l	Reactance of line l.
α_m, α_n	Participation rate of electrical and heat demands in multi-energy DRP.
β_r	Cost deviation factor.
λ^{co_2}	Carbon emission price.
Γ	Penalty price for wind curtailment.

II. Thermal units parameters:

a_i, b_i, c_i	Fuel function coefficient of unit i.
$\overline{P_i}$, $\underline{P_i}$	Maximum/minimum generation capacity of unit i.
RU_i, RD_i	Ramp-up/ramp-down limit of unit i.
sug_i, sdg_i	Start-up/shut-down fuel consumption of unit i.
T_i^{on}, T_i^{off}	Minimum on/off time of unit i.
λ_i^f	Flexible ramping reserve price of unit i.

III. Energy hub systems parameters:

A_{ch}	Efficiency of the heat exchanger.
COP_{ph}	Coefficient of P2H performance.
$GC^{\max}$	Maximum imported gas energy to energy hubs.
$\overline{H_q}$	Maximum heat generation capacity of CHP unit q.
$\overline{H_g}$, $\underline{H_g}$	Maximum/minimum heat generation capacity of gas boiler g.
$\overline{H_{ph}^{ch}}$, $\overline{H_{ph}^{dis}}$	Maximum heat generation/storing capacity of P2H ph.
$\overline{H_{ts}^{ch}}$, $\overline{H_{ts}^{dis}}$	Maximum heat generation/storing capacity of thermal storage ts.
$\overline{P_q}$, $\underline{P_q}$	Maximum/minimum power generation capacity of CHP unit q.
$\overline{P_{es}^{ch}}$, $\overline{P_{es}^{dis}}$	Maximum power generation/storing capacity of electrical storage es.
$\overline{P_{ph}}$	Maximum consumed power by P2H storage.

$\overline{S_{ph}}, \overline{S_{es}}, \overline{S_{ts}}$	Maximum stored energy of P2H ph, electrical storage es, thermal storage ts.
$\underline{S_{ph}}, \underline{S_{es}}, \underline{S_{ts}}$	Minimum stored energy of P2H ph, electrical storage es, thermal storage ts.
λ^{gas}	Gas price.
$\eta_i, \eta_q, \eta_g, \eta_{ph}$	Efficiency of thermal unit, CHP unit, gas boiler, P2H storage.
$\eta_{es}^{ch}, \eta_{es}^{dis}$	Efficiency of electrical storage in charge/discharge modes.
$\eta_{ts}^{ch}, \eta_{ts}^{dis}$	Efficiency of thermal storage in charge/discharge modes.
M	Sufficient large number.

Decision variables
I. General variables:
C_t^{dr}	Incentive compensation costs of multi-energy DRP at hour t.
$C_t^{co_2}$	Cost of CO_2 emissions at hour t.
C_t^{spill}	Cost of wind curtailment at hour t.
$EL_{m,t}^{dr}, HL_{n,t}^{dr}$	Final electrical and heat demands profile at hour t.
$PC_{w,t}$	Wind curtailment of wind farm w at hour t.
$PF_{l,t}$	Power flow on line l.
ξ	The horizon of the uncertain parameter.
$\delta_{s_l,t}, \delta_{e_l,t}$	Voltage angle on buses sl and el at hour t.
$\Delta E_{m,t}, \Delta H_{n,t}$	Electrical and heat loads curtailment after DRPs implementation at hour t.

II. Thermal units variables:
C_t^{th}	Operating cost of thermal units at hour t.
$F_i(P_{i,t})$	Cost function of unit i.
$P_{i,t}$	Power output of unit i at hour t.
$P_{i,t}^{ru}, P_{i,t}^{rd}$	Up/down flexible ramping reserves provided by unit i at hour t.
$SU_{i,t}, SD_{i,t}$	Start-up and shut-down costs of unit i at hour t.
$X_{i,t}^{on}, X_{i,t}^{off}$	On/off time of unit i at hour t.
$u_{i,t}, \nu_{i,t}, \gamma_{i,t}$	Binary variable to indicate status of thermal units.

III. Energy hub systems variables:
C_t^{hub}	Operating cost of energy hub systems at hour t.
$GC_{q,t}, GC_{g,t}$	Gas consumption by CHP unit q and gas boiler g at hour t.
$H_{q,t}, H_{g,t}$	Generated heat by CHP unit q and gas boiler g at hour t.
$H_{ph,t}^{ch}, H_{ph,t}^{dis}$	Heating stored/supplied by P2H storage ph at hour t.
$H_{ts,t}^{ch}, H_{ts,t}^{dis}$	Heating stored/supplied by thermal storage ts at hour t.
$HP_{ph,t}$	Generated heat by P2H storage ph at hour t.
$P_{q,t}$	Generated power by CHP unit q at hour t.
$P_{ph,t}$	Consumed power by P2H storage ph at hour t.
$P_{es,t}^{ch}, P_{es,t}^{dis}$	Electricity stored/supplied by electrical storage es at hour t.
$S_{ph,t}, S_{es,t}, S_{ts,t}$	Reservoir energy level of P2H ph, electrical storage es, thermal storage ts at hour t.
$u_{q,t}, u_{g,t}$	Binary variable to indicate status of CHP units, gas boilers.
$u_{ph,t}^{ch}, u_{ph,t}^{dis}$	Binary variables to indicate charge/discharge status of P2H ph.
$u_{es,t}^{ch}, u_{es,t}^{dis}$	Binary variables to indicate charge/discharge status of electrical storage es.
$u_{ts,t}^{ch}, u_{ts,t}^{dis}$	Binary variables to indicate charge/discharge status of thermal storage ts.

Functions
| $U(\tilde{P}_{w,t}, \xi)$ | Fractional uncertainty model in the IGDT approach. |
| $\tilde{\alpha}(X, TC_C)$ | Robustness function in the IGDT approach. |

1. Introduction

1.1. Motivation

Over the last decades, the electricity industry has undergone major changes in various sectors due to a number of structural, technical, and economic factors. Heightened concerns about nuclear power plants, energy prices, climate changes, and reliability requirements have led countries to increase the penetration of renewable energy sources (RESs) in the bulk power systems (Li et al. (2020)). Among the RESs, wind

units have attracted more attention and had the fastest growth around the world (Kong et al. (2018); Oskouei & Yazdankhah (2015)). At the end of 2019, the worldwide installed capacity of wind power reached 651 GW. The share of leading countries in the field of renewable energy, such as China, the United States, Germany, India, the United Kingdom, and Brazil in the global wind power capacity was equal to 33%, 16.08%, 9.89%, 5.86%, 3.46%, and 2.42%, respectively (GWEC (2019)).

From an environmental perspective, expansion planning of bulk power systems under high penetration of RESs brings many benefits to society. Perhaps the most prominent point is the reduction of greenhouse gas emissions (Behboodi et al. (2017)). Nevertheless, due to the aging of power grids infrastructure and non-uniformly distributed renewable sources, the use of the high-power intermittent RESs brings some technical challenges to the regional power system, such as line congestion (Chen et al. (2018)) and power balance violation (Deng & Lv (2020)). Because of these challenges, the control and protection systems may be obligated to reduce or curtail a large amount of generated renewable power. According to published statistics, at the end of 2019, the wind power curtailment was almost equal to 17.38 TWh in the power system worldwide (IEA (2019)). In addition, the power system operators have to pay high compensation costs to wind farm owners to curtail wind power. It can be observed that the existing power system structure is not suitable for hosting the high-penetration of RESs. Therefore, immediate actions supplemented with studies related to reducing power spillage of RESs are necessary today to prevent the waste of renewable energies.

1.2. Literature review

There are numerous research works that have investigated the existing challenges in power grids operation from different aspects considering the high penetration of RESs. The presented solutions in various literature can be divided into two categories from the energy vectors perspective.

I. First category: Research works included in this category analyzed the power grid in one-dimensional mode and the presented methods were focused solely on the sustainable performance of the bulk power system. The main approach governing this category was based on the use of optimal scheduling strategies for power grids operation in coordination with various technical tools, such as energy storage systems and demand response programs (DRPs). In addition, the power grids constraints were identified as a critical factor in advancing the objectives of these works. For instance, in (Wang et al. (2019a)), a multi-objective security-constrained unit commitment (SCUC) problem was established with the aim of analyzing the relationship between the rate of wind power curtailment and the system's operation cost. Furthermore, the developed scheduling model considered the impacts of utilizing energy storage systems and load shedding options on the power system operation process. In (Khaloie et al. (2020)), a scenario-based stochastic model was developed to optimally allocate energy storage systems in active power grids. The utilized structure aimed to harvest the maximum possible wind power by relying on the capabilities of the energy storage systems. A two-stage method was presented in (Dui et al. (2018)) by considering the role of thermal units, wind farms, and energy storage systems in the operation of power systems. In the first stage, the unit commitment (UC) problem was solved to determine the optimal scheduling of the generation units by relying on AC power flow constraints. The second stage

identified the appropriate operational strategy for energy storage systems. Authors of (Oskouei & Yazdankhah (2017)) suggested a promoted load shifting technique to maximize the utilization of RESs by considering the frequency-based pricing mechanism and pump-storage hydro plant. Moreover, in (Wang et al. (2018)), the energy management strategy was proposed for the optimal operation of microgrids based on the stochastic programming approach considering the high penetration of RESs. The utilized model in this work was formulated as a mixed-integer linear programming model and simulation results demonstrated that this model could reduce the power curtailment rate of RESs up to 12% and the total operational costs up to 17% compared to the initial state. In (Xie et al. (2018)), a multi-objective structure was used to achieve an optimal scheme of the bulk power system considering the high penetration of RESs. In (Xie et al. (2020a)), a two-stage robust optimization structure was presented to determine the optimal topology of urban transportation networks with the aim of minimizing the rate of curtailed renewable power.

Nevertheless, the impacts of the integrated energy system in reducing renewable power curtailment, compensating uncertainties of renewable power generation, decreasing the day-ahead operating costs, and increasing the flexibility and reliability of the power system were not considered in any of the aforementioned studies.

II. Second category: The studies included in this category made a step further by considering interdependency in a multi-vector energy community to alleviate or overcome the negative consequences of the integration of high-power RESs in power grids. The key requirements for upgrading the current power grid to the multidimensional mode were analyzed in these studies. In this regard, the energy hub system as an emerging concept in the context of the integrated multi-carrier energy systems was widely welcomed (Xie et al. (2020b)). Grid-connected energy hubs have a great potential for widespread integration of RESs as distributed means of generation to increase the energy efficiency and flexibility of the integrated energy systems (Dini et al. (2019)) as well as to reduce the waste of energy (Abdollahi & Lahdelma (2020)). These systems link independent natural gas and electricity networks at the subtransmission and distribution levels and then optimize them as an integrated system by relying on the energy conversion facilities such as combined heat and power (CHP), gas boiler (GB), and energy storage systems (Mohammadi et al. (2017)).

As stated in the literature, the optimization of the power grids operation in the presence of RESs, which follow the energy hub strategy was attracted much attention by the energy research community. Authors of (Eladl et al. (2020)) proposed a multi-objective optimization problem to minimize the overall costs of multiple energy hub systems. The uncertainties of both wind and photovoltaic systems were modeled by a scenario-based approach. Further, the effectiveness of energy storage systems to reduce wasted renewable energy was investigated and the overall energy losses were reduced up to 4% by the proposed method. In (Liang & Tang (2020)), the interval optimization framework was developed based on the UC problem and contingency issue in transmission lines to integrate power and natural gas networks with high penetration of wind power. The energy conversion facilities were utilized to reduce renewable power curtailment and provide auxiliary services for the power system operator. Authors of (Li et al. (2019)) introduced a decentral optimization framework to specify the optimal dispatch of the grid-connected energy hubs in

the framework of the hierarchical structure with a particular emphasis on RESs. The presented structure was modeled on the basis of the prevalent leader-followers relationships in integrated energy systems. The obtained results showed that the total operation cost of the integrated energy system was reduced by 7.24%. Authors of (Chen et al. (2015b)) provided a linear dispatch model to manage the energy flow stream in the integrated wind-CHP-heat storage system. The effects of energy conversion facilities on wind power curtailment were examined in a real power system located in North China. Numerical examples showed that energy conversion facilities could increase the flexibility of the integrated energy system and save 3.88% energy compared to the conventional system. However, the uncertainty of renewable generation was not addressed in the presented decision-making approaches in (Li et al. (2019); Chen et al. (2015b)). A recursive two-level optimization model was formulated in (Davatgaran et al. (2019)) to improve the interactions between the energy hub systems and the regional power system in the presence of wind units. In (Yan et al. (2019)), a robust day-ahead scheduling method was presented for high penetration of wind generation within the framework of multi-carrier energy networks. The main aim of this work was to minimize total operating costs and maximize the energy capture from the wind farms during the scheduling period. Moreover, in (Wang et al. (2019b)), an expansion planning model was investigated to determine the optimal operation of energy hubs in the framework of the multi-energy system by relying on the resource allocation problem.

According to the technical literature, all of the conducted studies in the second category have attempted to provide effective approaches for the optimal exploitation of power grids in coordination with energy hub systems and high-power RESs. In spite of the advances achieved in the utilization of the integrated energy systems, there are still some shortcomings that necessitate further research. The shortcomings (**Sh**) of the reviewed literature can be summarized as follows:

- **Sh1:** Lack of a holistic scheduling process in the above-mentioned studies to simultaneously optimize significant objectives such as operating costs, curtailed renewable power, and CO_2 emission factors. In fact, the main focus of most studies was on reducing the operating costs of the integrated energy system.

- **Sh2:** The effect of the up-to-date energy conversion facilities, such as power-to-heat (P2H) storage, in the form of energy hub systems was ignored in any of the aforementioned studies to determine the economical operation of the integrated energy system.

- **Sh3:** The benefits of multi-energy DRP were ignored in the relevant studies, as the efficient schemes that have the potential to increase the flexibility of the integrated energy system, reduce the operation costs, and decrease renewable power curtailment.

Table 1 categorizes the reviewed literature and provides the novelties of the proposed model in comparison to other researches.

1.3. Contributions and paper organization

To bridge these gaps, this paper presents a techno-economic-environmental approach to investigate the business and technical challenges of the multi-vector energy community that can be created by high-power RESs. The presented approach was formulated as a robust SCUC problem to optimally coordinate

Table 1: Comparison of the proposed strategy with existing methods in the related literature.

References	Scope of study	GHG emissions	Penalty for CRP	Resources				DRPs	Uncertainty modeling
				ECFs	RESs	ESSs	P2H		
(Wang et al. (2019a))	Bulk power system	-	-	-	✓	✓	-	Electrical DRPs	Stochastic
(Khaloie et al. (2020))	Bulk power system	✓	-	-	✓	✓	-	-	Stochastic
(Dui et al. (2018))	Bulk power system	-	✓	-	✓	✓	-	-	Stochastic
(Oskouei & Yazdankhah (2017))	Bulk power system	-	-	-	✓	✓	-	Electrical DRPs	Stochastic
(Wang et al. (2018))	Bulk power system	-	-	-	✓	✓	-	Electrical DRPs	Stochastic
(Xie et al. (2018))	Bulk power system	-	-	✓	✓	✓	-	-	Probabilistic
(Xie et al. (2020a))	Bulk power system	-	✓	✓	✓	✓	-	-	Probabilistic
(Eladl et al. (2020))	Multi-energy system	✓	-	✓	✓	✓	-	-	Stochastic
(Liang & Tang (2020))	Multi-energy system	-	-	✓	✓	✓	-	-	Fuzzy logic approach
(Li et al. (2019))	Multi-energy system	-	-	✓	✓	✓	-	-	Deterministic
(Chen et al. (2015b))	Multi-energy system	-	-	✓	✓	✓	-	-	Deterministic
(Davatgaran et al. (2019))	Multi-energy system	-	-	✓	✓	✓	-	Multi-energy DRPs	Stochastic
(Yan et al. (2019))	Multi-energy system	-	✓	✓	✓	✓	-	-	Robust
(Wang et al. (2019b))	Multi-energy system	-	-	✓	✓	✓	-	-	Probabilistic
Proposed model	Multi-energy system	✓	✓	✓	✓	✓	✓	Multi-energy DRPs	IGDT

*Note: GHG-Greenhouse gas; CRP-Curtailed renewable power; ECFs-Energy conversion facilities; ESSs-Energy storage systems

the operation of the regional power system with the grid-connected energy hubs by relying on the high penetration of wind power. Grid-connected energy hubs, which were equipped with CHP unit, GB unit, electrical energy storage (EES), thermal energy storage (TES), and P2H storage, were the principal entity in the developed scheduling process to reach the desired objectives. Briefly, the outstanding objectives of this work are to increase the flexibility of the integrated energy system, minimize the total operating costs of the integrated energy system, decrease the amount of curtailed wind power, and reduce the CO_2 emission rate.

Furthermore, an information-gap decision theory (IGDT)-based robust decision-making method was proposed to handle wind power uncertainty. The presented IGDT-based robust SCUC approach with energy storage systems and multi-energy DRP as the flexibility resources were used to reduce the effect of wind power uncertainty on the flexibility and costs of the integrated energy system. Accordingly, the main contributions of this paper are summarized as follow:

- A holistic scheduling process was presented to determine the optimal operation of the regional power system by relying on the grid-connected energy hubs. In the proposed structure, the role of CO_2 emissions, renewable power curtailment, and multi-energy DRP implementation was intended in the total operating cost (to tackle **Sh1**).

- The IGDT-based robust SCUC model was presented to reach the robustness function with regards to the uncertainty of wind power.

- The prevalent energy hub systems were equipped with up-to-date energy conversion facilities like P2H storage, to harness the actual arbitrage opportunities in different layers of the multi-vector

energy community (to tackle **Sh2**).

- The role of incentive-based multi-energy DRP implementation was investigated in decreasing total operation costs and wind power curtailment, considering fair rewards (to tackle **Sh3**).

The remainder of this paper is structured as follows. The description of the presented strategy is given in Section 2. The methodology and mathematical formulation of the IGDT-based robust SCUC problem are provided in Section 3. In Section 4, various case studies are defined to evaluate the effectiveness of this research, and obtained results are discussed later in Section 5. Finally, conclusions and future work are given in Section 6.

2. The proposed framework

This paper proposes an IGDT-based robust SCUC approach for the optimal exploitation of the regional power system in the presence of grid-connected energy hubs and high-power wind farms. Establishing an appropriate connection between the regional power systems and energy hub systems enables operators to utilize the capacity of other energy systems such as the natural gas network in addition to the power grid infrastructure. This mechanism creates many economic opportunities for the power system operator in energy markets and helps the operator to reduce wind power curtailment, increase the system flexibility, and fulfill its obligations at the lowest operating cost. The framework of the proposed structure is shown in Fig. 1. Since the proposed structure is drawn up from the perspective of the regional power system, the power system operator is responsible for the optimal exploitation of the integrated energy system. The integrated energy system consists of thermal units, wind farms, and large-scale energy hubs. In the integrated energy system, the regional power system operator uses the ability of the grid-connected energy hubs like a multi-carrier energy generation/storage unit. Hence, the cost of energy exchanged between grid-connected energy hubs and the regional power system is not considered in the mathematical formulation.

As shown in Fig. 1, the input ports of energy hubs are connected to the natural gas network and regional power system. The natural gas is bought from the upstream network by the regional power system operator. The output ports of energy hubs can be connected to the energy demands of large industrial parks or district energy networks. It should be noted that in the proposed structure, despite accurate modeling of the regional power system and energy hubs' equipment, dynamic modeling of natural gas and district heating networks were ignored. However, the concept of gas and heat energy flow was considered on buses where the energy hubs were connected to the regional power system.

Besides, the impacts of the multi-energy DRP as a practical flexibility option were investigated to harvest higher wind power as well as to reduce operating costs of the integrated energy system. DRPs provide special opportunities for different institutions such as aggregators, system operators, transmission planners, and customers to play a significant role in the operation of the regional power system. DRPs can also be used by the transmission network planner as resource options to create suitable planning and increase the system's stabilities. In this paper, the incentive-based multi-energy DRP based on the load curtailment option was used to apply the desired control strategies.
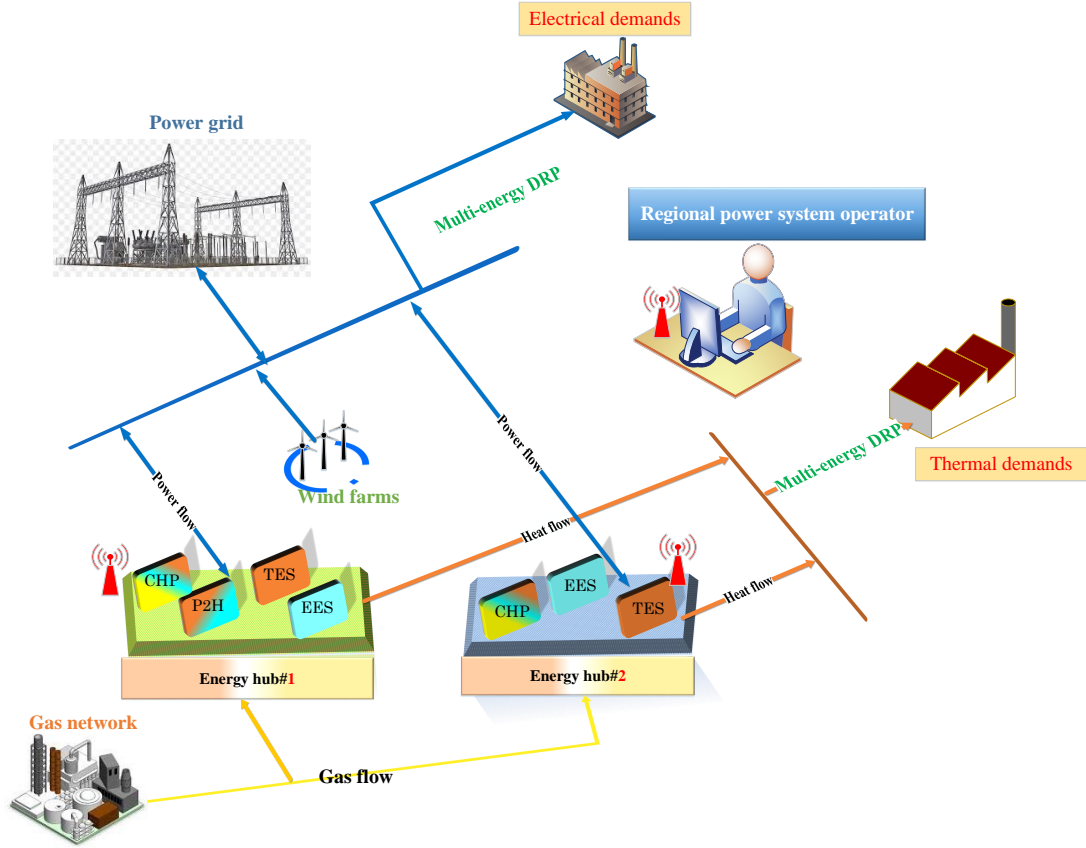
8

Fig. 1: The presented structure to upgrade regional power system in the form of integrated energy system.

The presented IGDT-SCUC approach will be evaluated under different conditions in the context of the robustness optimization problem. The main attitude toward solving the constructed robustness optimization problem is to minimize the total operating costs of the integrated energy system, renewable power curtailment, and greenhouse gas emissions. To achieve these targets, the integrated energy system operation should be improved by optimal utilization of grid-connected energy hubs, optimizing energy management, and increasing the utilization of wind farms. How to deal with the proposed optimization problem is described in detail in Section 3.

3. Problem formulation

This section presents the optimal scheduling process of the integrated energy system consisting of the regional power system and grid-connected energy hubs in the presence of the high-power wind farms. In the following sub-sections, objective function, the model of various components of the integrated energy system, and all the required constraints are expressed.

3.1. Objective function

The deterministic SCUC model to make optimum utilization of the regional power system in the coordinated with grid-connected energy hubs can be formulated as (1), where wind farms output power is considered as forecasted values. The objective function of the proposed model corresponds to minimizing the total cost (TC) of integrated energy system operation. Therefore, the objective function can be

formulated as follows.

$$Min: \quad TC = \sum_{t=1}^{NT} \left[C_t^{th} + C_t^{hub} + C_t^{CO_2} + C_t^{spill} + C_t^{dr} \right] \tag{1}$$

The objective function is composed of five terms: 1) operating cost of thermal units (C_t^{th}); 2) operating cost of individual energy hub systems (C_t^{hub}); 3) cost of CO_2 emission rate ($C_t^{CO_2}$); 4) cost of wind power curtailment (C_t^{spill}); 5) compensation costs to implement the multi-energy DRP (C_t^{dr}). Each component of the objective function is formulated to perform the SCUC model as follows.

3.2. Thermal units modeling

The operation cost of thermal units, given in (2), consists of three parts considering the integrated energy system constraints: 1) the fixed and variable costs of generating electricity which is given by (3); 2) the flexible ramping cost; 3) the start-up and shut-down costs.

$$C_t^{th} = \sum_{i=1}^{NI} \left[u_{i,t} \cdot \left(F_i(P_{i,t}) + \lambda_i^f \cdot (P_{i,t}^{ru} + P_{i,t}^{rd}) \right) + SU_{i,t} + SD_{i,t} \right] \tag{2}$$

$$F_i(P_{i,t}) = a_i P_{i,t}^2 + b_i P_{i,t} + c_i \tag{3}$$

The values of up/down flexible ramping reserve provided by each thermal unit are directly correlated with the unloaded power capacity. The corresponding limitations are given in (4) and (5). Furthermore, (6) and (7) ensure that the assigned values to the flexible reserves do not exceed the permissible limits during the scheduling intervals.

$$P_{i,t} + P_{i,t}^{ru} \le \overline{P_i} \cdot u_{i,t} \ , \quad \forall i,t \tag{4}$$

$$P_{i,t} - P_{i,t}^{rd} \ge \underline{P_i} \cdot u_{i,t} \ , \quad \forall i,t \tag{5}$$

$$0 \le P_{i,t}^{ru} \le RU_i \ , \quad \forall i,t \tag{6}$$

$$0 \le P_{i,t}^{rd} \le RD_i \ , \quad \forall i,t \tag{7}$$

The constraints of the thermal units ramp-rates in the consecutive period should be satisfied by (8)-(11), in which the binary variables are equal to 1 if each unit is in the on mode, otherwise, it will be zero.

$$P_{i,t} - P_{i,t-1} + P_{i,t}^{ru} \le (1 - \nu_{i,t}) \cdot RU_i + \underline{P_i} \cdot \nu_{i,t} \ , \quad \forall i,t \tag{8}$$

$$P_{i,t-1} - P_{i,t} + P_{i,t}^{rd} \le (1 - \gamma_{i,t}) \cdot RD_i + \underline{P_i} \cdot \gamma_{i,t} \ , \quad \forall i,t \tag{9}$$

$$\nu_{i,t} - \gamma_{i,t} = u_{i,t} - u_{i,t-1} \ , \quad \forall i,t \tag{10}$$

$$\nu_{i,t} + \gamma_{i,t} \ge 1 \ , \quad \forall i,t \tag{11}$$

The start-up and shut-down costs of each thermal unit can be calculated by (12) and (13).

$$SU_{i,t} \ge sug_i \cdot (u_{i,t} - u_{i,t-1}); \quad SU_{i,t} \ge 0 \ , \quad \forall i,t \tag{12}$$

$$SD_{i,t} \geq sdg_i \cdot (u_{i,t-1} - u_{i,t}); \quad SD_{i,t} \geq 0 \quad , \quad \forall i,t \tag{13}$$

Equations (14) and (15) indicate the minimum up/down time limits for each thermal unit, respectively.

$$(X_{i,t-1}^{on} - T_i^{on}) \cdot (u_{i,t-1} - u_{i,t}) \geq 0 \ , \quad \forall i,t \tag{14}$$

$$(X_{i,t-1}^{off} - T_i^{off}) \cdot (u_{i,t} - u_{i,t-1}) \geq 0 \ , \quad \forall i,t \tag{15}$$

3.3. Energy hub systems modeling

Each grid-connected energy hub contains a variety of energy conversion facilities to cover electricity and heat demands while interacting with the regional power system. The operation cost of the individual energy hub systems that are in coordination with the regional power system depends only on the amount of purchased gas from the natural gas network as well as natural gas prices. In this study, the energy hub systems are equipped with CHP, GB, P2H, EES, and TES units. Therefore, CHP and GB units are the only elements that make up the operating cost of energy hub systems. This concept is shown in (16). The operational constraints related to each component of energy hub systems are explained below. It should be noted that, in the proposed SCUC optimization model, the energy hub systems can be easily extended to include other conversion facilities.

$$C_t^{hub} = \sum_{g=1}^{NG} \sum_{q=1}^{NQ} \lambda^{gas} \cdot (GC_{q,t} + GC_{g,t}) \ , \quad \forall t \tag{16}$$

3.3.1. CHP unit

The heat and power generation of the CHP unit are interdependent and expressed by a boundary curve ABCD, as shown in Fig. 2. According to this figure, the relationship between output heat and power can be described by three linear inequalities, as given in (17)-(19). In addition, the power and heat production of the CHP unit at each interval should be within the lower and upper limits, as shown in (20) and (21). Moreover, the amount of natural gas purchased from the gas network for the uninterrupted operation of the CHP unit can be calculated by (22).

$$P_{q,t} - P_{q,A} - \frac{P_{q,A} - P_{q,B}}{H_{q,A} - H_{q,B}} \cdot (H_{q,t} - H_{q,A}) \leq 0 \ , \quad \forall q,t \tag{17}$$

$$P_{q,t} - P_{q,B} - \frac{P_{q,B} - P_{q,C}}{H_{q,B} - H_{q,C}} \cdot (H_{q,t} - H_{q,B}) \geq -(1 - u_{q,t}) \cdot M \ , \quad \forall q,t \tag{18}$$

$$P_{q,t} - P_{q,C} - \frac{P_{q,C} - P_{q,D}}{H_{q,C} - H_{q,D}} \cdot (H_{q,t} - H_{q,C}) \geq -(1 - u_{q,t}) \cdot M \ , \quad \forall q,t \tag{19}$$

$$\underline{P_q} \cdot u_{q,t} \leq P_{q,t} \leq \overline{P_q} \cdot u_{q,t} \ , \quad \forall q,t \tag{20}$$

$$0 \leq H_{q,t} \leq \overline{H_q} \cdot u_{q,t} \ , \quad \forall q,t \tag{21}$$

$$GC_{q,t} = \frac{P_{q,t}}{\eta_q} \ , \quad \forall q,t \tag{22}$$
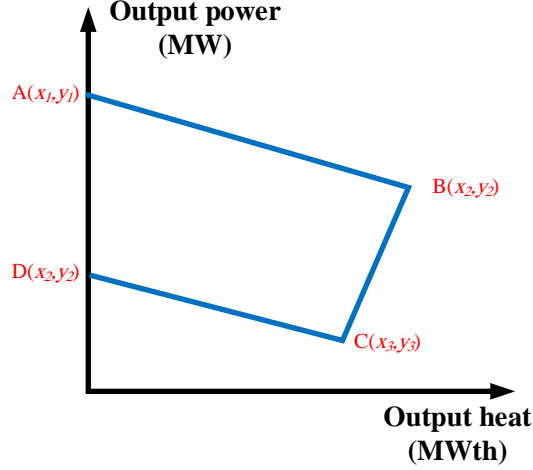
Fig. 2: Operation region of CHP unit.

3.3.2. GB unit

Equation (23) sets upper and lower bounds for heat generation from the GB unit at any hour of scheduling horizon. Also, the amount of injected natural gas into the GB unit with regards to the thermal efficiency of each unit can be calculated by (24).

$$\underline{H_g} \cdot u_{g,t} \leq H_{g,t} \leq \overline{H_g} \cdot u_{g,t} \quad , \quad \forall g,t \tag{23}$$

$$GC_{g,t} = \frac{H_{g,t}}{\eta_g} \quad , \quad \forall g,t \tag{24}$$

3.3.3. P2H storage

The technical and operational constraints for the exploitation of different types of P2H systems, such as heat pumps, are presented in (25)-(32). Based on (25), the level of stored heat energy in the P2H storage at time t is a function of the reserved energy at time t-1, the injected heat energy to the reservoir at time t, and the delivered heat energy to the integrated energy system at time t. In order to protect the P2H reservoir, the stored heat energy should be limited in the permissible range, which is reflected in inequality (26). Based on (27), the stored heat energy in the P2H reservoir in the first ($t = 0$) and last ($t = NT$) scheduling intervals should be equal. The heat charging and discharging rates of the P2H storage are limited as presented in (28) and (29). Equation (30) shows that the produced heat by the P2H storage can be delivered to the integrated energy system or stored in the reservoir. Also, the consumed power by the P2H storage should be limited in the allowed range which is shown in (31). Equation (32) guarantees that the P2H storage cannot be charged and discharged simultaneously.

$$S_{ph,t} = (1 - \eta_{ph})S_{ph,t-1} + H_{ph,t}^{ch} - H_{ph,t}^{dis} \quad , \quad \forall ph,t \tag{25}$$

$$\underline{S_{ph}} \leq S_{ph,t} \leq \overline{S_{ph}} \quad , \quad \forall ph,t \tag{26}$$

$$S_{ph,0} = S_{ph,NT} \quad , \quad \forall ph \tag{27}$$

$$0 \leq H_{ph,t}^{ch} \leq \overline{H_{ph}^{ch}} \cdot u_{ph,t}^{ch} \quad , \quad \forall ph,t \tag{28}$$

$$0 \leq H_{ph,t}^{dis} \leq \overline{H_{ph}^{dis}} \cdot u_{ph,t}^{dis} \quad , \quad \forall ph, t \tag{29}$$

$$H_{ph,t}^{ch} + HP_{ph,t} = COP_{ph} \cdot P_{ph,t} \quad , \quad \forall ph, t \tag{30}$$

$$0 \leq P_{ph,t} \leq \overline{P_{ph}} \quad , \quad \forall ph, t \tag{31}$$

$$u_{ph,t}^{ch} + u_{ph,t}^{dis} \leq 1 \quad , \quad \forall ph, t \tag{32}$$

3.3.4. EES system

The technical and operational constraints of the EES system are described as follows.

$$S_{es,t} = S_{es,t-1} + \eta_{es}^{ch} \cdot P_{es,t}^{ch} - \frac{P_{es,t}^{dis}}{\eta_{es}^{dis}} \quad , \quad \forall es, t \tag{33}$$

$$\underline{S_{es}} \leq S_{es,t} \leq \overline{S_{es}} \quad , \quad \forall es, t \tag{34}$$

$$S_{es,0} = S_{es,NT} \quad , \quad \forall es \tag{35}$$

$$0 \leq P_{es,t}^{ch} \leq \overline{P_{es}^{ch}} \cdot u_{es,t}^{ch} \quad , \quad \forall es, t \tag{36}$$

$$0 \leq P_{es,t}^{dis} \leq \overline{P_{es}^{dis}} \cdot u_{es,t}^{dis} \quad , \quad \forall es, t \tag{37}$$

$$u_{es,t}^{ch} + u_{es,t}^{dis} \leq 1 \quad , \quad \forall es, t \tag{38}$$

The electrical energy balance constraint of the EES system is given by (33). The same as the P2H storage, the stored electrical energy of the EES system should be limited in a certain range, which is given by (34). Similar to other energy storage systems, the level of the electrical energy reservoir at the end of the scheduling time horizon should be equal to the initial level of the reservoir, which is stated as (35). Based on (36) and (37), each EES system should be charged or discharged within the upper and lower limits. Inequality (38) guarantees that the EES system cannot be charged and discharged simultaneously.

3.3.5. TES system

The technical and operational constraints of the TES system include the level of the thermal energy reservoir, limits on the reservoir and charging/discharging thermal energy, plus constraint to prevent simultaneous charging and discharging. Equations (39)-(44) show the relevant constraints.

$$S_{ts,t} = S_{ts,t-1} + \eta_{ts}^{ch} \cdot H_{ts,t}^{ch} - \frac{H_{ts,t}^{dis}}{\eta_{ts}^{dis}} \quad , \quad \forall ts, t \tag{39}$$

$$\underline{S_{ts}} \leq S_{ts,t} \leq \overline{S_{ts}} \quad , \quad \forall ts, t \tag{40}$$

$$S_{ts,0} = S_{ts,NT} \quad , \quad \forall ts \tag{41}$$

$$0 \leq H_{ts,t}^{ch} \leq \overline{H_{ts}^{ch}} \cdot u_{ts,t}^{ch} \quad , \quad \forall ts, t \tag{42}$$

$$0 \leq H_{ts,t}^{dis} \leq \overline{H_{ts}^{dis}} \cdot u_{ts,t}^{dis} \quad , \quad \forall ts, t \tag{43}$$

$$u_{ts,t}^{ch} + u_{ts,t}^{dis} \leq 1 \quad , \quad \forall ts, t \tag{44}$$

3.4. Carbon emission modeling

In the desired integrated energy system, thermal units consume fossil fuels to produce electrical power. Meanwhile, CHP and GB units consume natural gas to produce heat and/or electricity. The rates of CO_2 emission for energy sources that use fossil fuels can be defined by dividing the CO_2 emissions factor by the efficiencies of the various resource types. According to this issue, the CO_2 emission cost of the integrated energy system is defined as follows.

$$C_t^{co_2} = \lambda^{co_2} \cdot \left[\sum_{i=1}^{NI} em_i \cdot \left(\frac{P_{i,t} + P_{i,t}^{ru} - P_{i,t}^{rd}}{\eta_i} \right) + \sum_{q=1}^{NQ} em_q \cdot \left(\frac{A_{ch} \cdot P_{q,t}}{\eta_q} \right) + \sum_{g=1}^{NG} \frac{em_g \cdot H_{g,t}}{\eta_g} \right], \quad \forall t \qquad (45)$$

3.5. Wind power curtailment modeling

In order to simultaneously study the technical and economic challenges posed by high wind power penetration in the integrated energy system, the cost of wind power curtailments is considered in the provided structure. Equation (46) shows the wind power curtailment cost. Where constraint (47) is the amount of wind power curtailment in each wind farm at each time interval, which should be lower than the forecasted wind power of each wind farm.

$$C_t^{spill} = \sum_{w=1}^{NW} \Gamma \cdot PC_{w,t}, \quad \forall t \qquad (46)$$

$$0 \leq PC_{w,t} \leq P_{w,t}, \quad \forall t, w \qquad (47)$$

3.6. Integrated energy system constraints

In this study, the integrated energy system is fed by upstream electricity and natural gas networks as well as wind farms. The output of the integrated energy system can meet the electrical and heat demands in district energy networks. The electrical demands of district networks are met by the wholesale electricity market, wind farms, and the existed energy conversion facilities in the grid-connected energy hub systems. Meanwhile, the heat demands of district networks are met by CHP units, GB units, P2H storages, and TES systems, which are located in the grid-connected energy hub systems. Hence, the energy balance constraints for electrical and heat demands in the integrated energy system can be described by Kirchoff's first law, which is presented in (48) and (49). These equations guarantee the energy balance at bus b at each scheduling interval. In addition, the constraint of the gas flow for the grid-connected energy hubs is shown in (50).

$$\sum_{i=1}^{NI} KI_{b,i} \cdot P_{i,t} + \sum_{w=1}^{NW} KW_{b,w} \cdot P_{w,t} + \sum_{q=1}^{NQ} KQ_{b,q} \cdot P_{q,t} +$$
$$\sum_{es=1}^{NES} KE_{b,es} \cdot (P_{es,t}^{dis} - P_{es,t}^{ch}) - \sum_{w=1}^{NW} KW_{b,w} \cdot PC_{w,t} - \qquad (48)$$
$$\sum_{ph=1}^{NPH} KP_{b,ph} \cdot P_{ph,t} - \sum_{m=1}^{NM} KM_{b,m} \cdot EL_{m,t}^{dr} = \sum_{l=1}^{NL} KL_{b,l} \cdot PF_{l,t}, \quad \forall b, t$$

$$\sum_{q=1}^{NQ} KQ_{b,q} \cdot H_{q,t} + \sum_{g=1}^{NG} KG_{b,g} \cdot H_{g,t} + \sum_{ph=1}^{NPH} KP_{b,ph} \cdot (H_{ph,t}^{dis} - H_{ph,t}^{ch} + HP_{ph,t})$$
$$+ \sum_{ts=1}^{NTS} KT_{b,ts} \cdot (H_{ts,t}^{dis} - H_{ts,t}^{ch}) = \sum_{n=1}^{NN} KN_{b,n} \cdot HL_{n,t}^{dr}, \quad \forall b, t \qquad (49)$$

14

$$0 \leq \sum_{g=1}^{NG} \sum_{q=1}^{NQ} \left(GC_{q,t} + GC_{g,t} \right) \leq GC^{\max} \quad , \quad \forall t \tag{50}$$

In the regional power system, the power flow limits are enforced using the DC power flow model. Constraints (51)-(53) denote the transmission line power flow (from bus s_l to bus e_l), angle of the slack bus, and capacity of each line.

$$PF_{l,t} = \frac{\delta_{s_l,t} - \delta_{e_l,t}}{x_l} \quad , \quad \forall l,t \tag{51}$$

$$\delta_{slack,t} = 0 \quad , \quad \forall t \tag{52}$$

$$-\overline{F_l} \leq PF_{l,t} \leq \overline{F_l} \quad , \quad \forall l,t \tag{53}$$

Finally, the power system up/down flexible ramping reserves requirements at each time interval are limited according to (54).

$$\begin{cases} \sum_{i=1}^{NI} P_{i,t}^{ru} \geq FR_t^{up} \quad , \quad \forall t \\ \sum_{i=1}^{NI} P_{i,t}^{rd} \geq FR_t^{dw} \quad , \quad \forall t \end{cases} \tag{54}$$

3.7. Multi-energy demand response

The principal goals of using multi-energy DRP are to maximize the utilization of wind power and minimize the total operating costs of the integrated energy system. In this study, multi-energy DRP was considered to manage the electrical and heat demands' behavior with respect to the incentive-based demand response model. In order to encourage as many different consumers as possible to participate in the multi-energy DRP, it is imperative to dedicate the incentive compensation costs (inconvenience cost of subscribers) as the fair rewards to the various consumers. It should be noted that in this paper, the incentive-based demand response model was performed based on the load curtailment option. Therefore, the incentive compensation costs paid to the different types of energy consumers in order to implement the multi-energy DRP can be defined as (55).

$$C_t^{dr} = \sum_{n=1}^{NN} \sum_{m=1}^{NM} \left[\left(IE \times \left| \Delta E_{m,t} \right| \right) + \left(IH \times \left| \Delta H_{n,t} \right| \right) \right] \tag{55}$$

Based on (56) and (57), the load curtailment program is performed on the electrical and heat demands with regard to the participation rate of each consumer. Finally, the final electrical and heat profiles can be calculated by (58) and (59) according to the rate of changes in the initial energy demands.

$$\left| \Delta E_{m,t} \right| \leq \alpha_m \times EL_{m,t}^{ini} \quad , \quad \forall m,t \tag{56}$$

$$\left| \Delta H_{n,t} \right| \leq \alpha_n \times HL_{n,t}^{ini} \quad , \quad \forall n,t \tag{57}$$

15

$$EL_{m,t}^{dr} = \Delta E_{m,t} + EL_{m,t}^{ini} \quad \forall m,t \tag{58}$$

$$HL_{n,t}^{dr} = \Delta H_{n,t} + HL_{n,t}^{ini} \quad \forall n,t \tag{59}$$

3.8. IGDT-based robust SCUC model

The uncertainty of wind power poses many technical challenges for the optimal operation of the regional power system in the presence of the grid-connected energy hubs. Therefore, it is important to adopt a proper method to deal with the uncertainty of wind power. In this paper, the IGDT-based robust SCUC approach was employed to handle wind power uncertainty and reduce the impacts of wind power uncertainty on the flexibility and costs of the integrated energy system. Unlike stochastic models, the IGDT method is a non-probabilistic approach and does not need any fuzzy logic membership or probability distribution function (PDF) (Mohammadi-Ivatloo et al. (2013)). To tackle the uncertainty of wind power, the IGDT approach can be explained by two different strategies: risk-seeker and risk-averse strategies. In this study, the risk-averse strategy was utilized to make the integrated energy system robust against the uncertainties. This action will increase the operating costs compared to the deterministic condition. In the IGDT-based robust approach (risk-averse strategy), the main aim is to maximize the acceptable range of the wind power production uncertainty by adjusting various decision variables to guarantee an acceptable amount of the operating cost with regards to the predefined value for the objective function. The general model of the IGDT-based robust optimization problem was presented in (Chen et al. (2015a); Soroudi et al. (2017); Mirzaei et al. (2019)). Fig. 3 illustrates how the IGDT-based robust approach works. As shown in this figure, the system operator aims to extend the tolerable uncertainty of wind power generation (depicted as ξ in X-axis), by finding the optimal settings for the various decision variables.
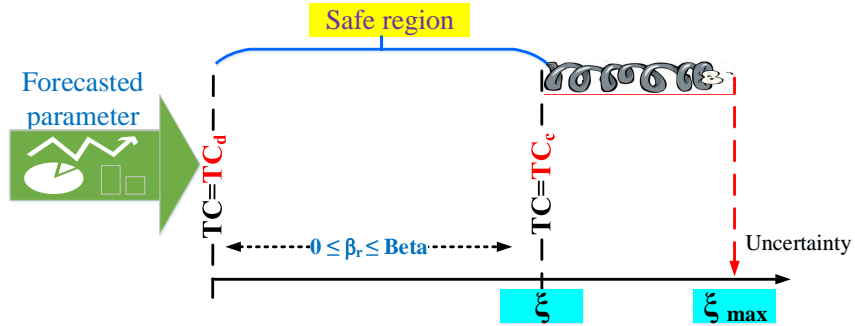

Fig. 3: Illustrating of the IGDT-based robust approach.

In the proposed structure, wind power $(P_{w,t})$ is an uncertain parameter and the envelope bound model is applied to describe the required information about $P_{w,t}$, as follows (Majidi et al. (2019)):

$$U(\tilde{P}_{w,t}, \xi) = \left\{ P_{w,t} : \left| \frac{P_{w,t} - \tilde{P}_{w,t}}{\tilde{P}_{w,t}} \right| \leq \xi \right\}, \quad \xi \geq 0 \tag{60}$$

Where $\tilde{P}_{w,t}$ is the forecasted value of the uncertain parameter $P_{w,t}$, and ξ is the unknown horizon of uncertainty for decision making. The use of the IGDT-based robust strategy will help the regional system operator to schedule in a way that is immune to higher costs. The mathematical formulation of

16

the IGDT-based robust SCUC model can be stated as (61) and (62).

$$\tilde{\alpha}(X, TC_C) = \max \left\{ \xi : \left(\max_{P_{w,t}} \quad TC \leq TC_C \right) \right\} \tag{61}$$

$$TC_C = (1 + \beta_r) \cdot TC_d \tag{62}$$

Where TC_C is the acceptable level of cost target for the robustness function and TC_d is the base level of the objective function. Furthermore, β_r represents the cost deviation factor of the base case value and X denotes the set of various decision variables. In different energy markets, the acceptable level of cost target (i.e., TC_C) depends on several issues such as reliability indices, social welfare index, and economic subjects. In the IGDT-based robust model, energy market operators can achieve the desired goals by adjusting β_r as input to the simulation program.

As can be seen, equations (60)-(62) constitute a bi-level optimization problem. The bi-level problem can be converted to a single-level problem using an innovative approach. It is clear that reducing the output power of wind farms will have an undesirable impact on the performance of the integrated energy system and will cause the system operator to incur higher costs for operating the regional power system. Therefore, in this model, only the reduction of wind power is considered as the forecast error. Therefore, to convert the bi-level problem to the single-level problem, the following assumptions must be considered in the IGDT-base robust SCUC model:

1: It is clear that if the wind power generation is lower than the forecasted value, the total operation cost of the integrated energy system will increase. Therefore, only the power reduction of wind farms should be considered in the scheduling process ($P_{w,t} = (1 - \xi) \cdot \tilde{P}_{w,t}$).

2: To reach a robust approach, the amount of wind power curtailment should be adjusted as follows. $0 \leq PC_{w,t} \leq (1 + \xi) \cdot \tilde{P}_{w,t}$.

Consequently, the IGDT-based robust SCUC model in the form of a single-level problem can be presented as follows.

$$\tilde{\alpha} = \max \xi \tag{63}$$

$$\sum_{t=1}^{NT} \left[C_t^{th} + C_t^{spill} + C_t^{hub} + C_t^{co_2} + C_t^{dr} \right] \leq (1 + \beta_r) \cdot TC_d \tag{64}$$

$$
\begin{aligned}
&\sum_{i=1}^{NI} KI_{b,i} \cdot P_{i,t} + \sum_{w=1}^{NW} KW_{b,w} \cdot (1 - \xi) \cdot \tilde{P}_{w,t} + \sum_{q=1}^{NQ} KQ_{b,q} \cdot P_{q,t} + \\
&\sum_{es=1}^{NES} KE_{b,es} \cdot (P_{es,t}^{dis} - P_{es,t}^{ch}) - \sum_{w=1}^{NW} KW_{b,w} \cdot PC_{w,t} - \sum_{ph=1}^{NPH} KP_{b,ph} \cdot P_{ph,t} - \\
&\sum_{m=1}^{NM} KM_{b,m} \cdot EL_{m,t}^{dr} = \sum_{l=1}^{NL} KL_{b,l} \cdot PF_{l,t}, \quad \forall b, t
\end{aligned} \tag{65}
$$

$$0 \leq PC_{w,t} \leq (1 + \xi) \cdot \tilde{P}_{w,t} \tag{66}$$

$$s.t. \quad (2) - (46) \quad and \quad (49) - (59) \tag{67}$$

The complete set of equations that make up the proposed model is given in Table 2.

Table 2: The complete set of equations making up the IGDT-based robust SCUC model.

	Objective function	Maximize: ξ
	Subject to:	(2), (3), (16), (45), (46), (55), (64)
Operational & technical constraints	Thermal units modeling	(4)-(15)
	CHP units modeling	(17)-(22)
	GB units modeling	(23), (24)
	P2H storages modeling	(25)-(32)
	EES systems modeling	(33)-(38)
	TES systems modeling	(39)-(44)
	Integrated energy system	(49)-(54), (65), (66)
	Multi-energy DRPs modeling	(56)-(59)

4. Model implementation and case studies

The proposed IGDT-based robust SCUC model for optimal operation of the regional power system in coordination with grid-connected energy hubs and high-power wind farms was implemented on a modified 6-bus test system. After that, the proposed model was applied to a modified 24-bus test system to show that the proposed approach is comprehensive. To scrutinize the influence of energy storage systems and multi-energy DRP on test systems, the following case studies were considered:

Case1: The deterministic SCUC model was applied to the regional power system by considering energy hub systems and without wind power uncertainty. In this case, energy hub systems were only equipped with CHP and GB units. This case study was considered as the **base case**.

Case2: The P2H storage, EES, and TES were plugged into existing energy hub systems, and then the impacts of these technologies on case 1 were investigated.

Case3: The effect of multi-energy DRP on case 2 was investigated.

Case4: The IGDT-based robust SCUC model was implemented for cases 1 and 3.

A technical and economical comparison between these case studies can well illustrate the objectives of the proposed structure. Important technical, economic, and environmental aspects of the proposed structure, which can be achieved through technical simulation, are as follows:

(1) Determining the hourly energy dispatch of each energy production unit for each case study; (2) calculating the rate of curtailed wind power for each case study; (3) analyzing the electrical and heat demands profile after implementing the multi-energy DRP; (4) evaluating the total operation cost and locational marginal price (LMP) for each case study; and (5) investigating the effect of wind power uncertainty in the scheduling process. An overview of the simulation process and key outcomes of the proposed structure is shown in Fig. 4.

The proposed model was coded as the mixed-integer nonlinear programming (MINLP) optimization problem in the general algebraic modeling system (GAMS). The scheduling horizon was set to be one day, and then the entire time horizon (NT) was partitioned into 24 periods. The considered case studies were conducted using DICOPT solver under GAMS software on a personal computer with CPU: 2.4 GHz

and RAM: 6 GB. The computational time of the proposed optimization problem for the final state of modeling (**Case 4**) is about 68 seconds and 139 seconds for the 6-bus test system and 24-bus test system, respectively.
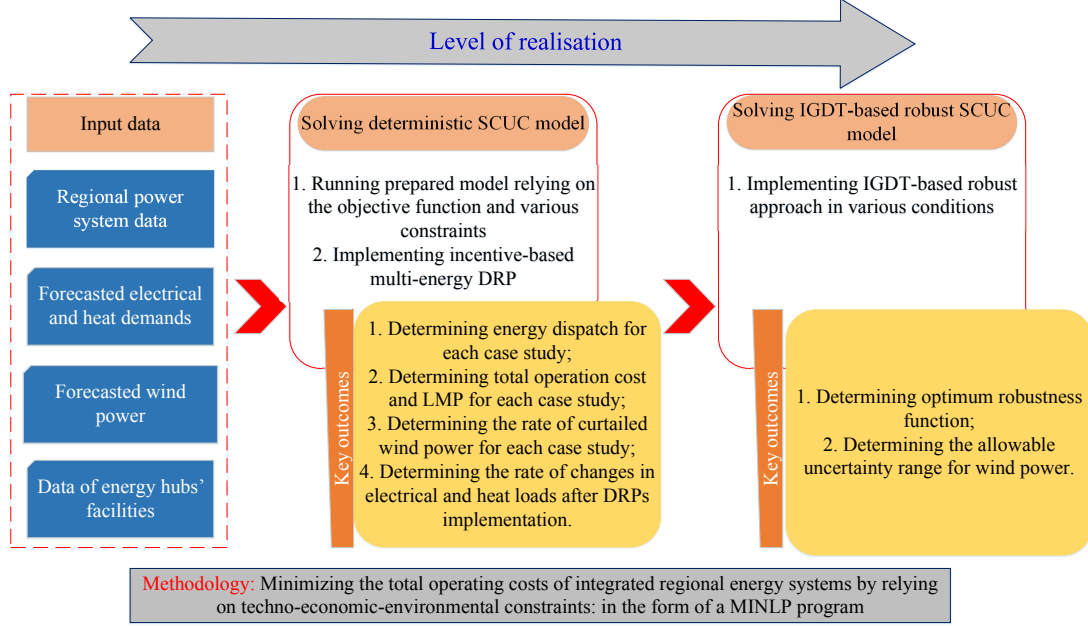

Fig. 4: The proposed structure.

5. Simulation results and discussion

5.1. Modified 6-bus test system

The topology of the modified 6-bus test system is illustrated in Fig. 5. This system has three regular thermal units, seven transmission lines, one wind farm, two energy hub systems, three electrical loads, and two heat loads. It should be noted that the buses of the wind farm and energy hub systems were selected arbitrarily. To use the proposed model to determine the optimal coordinated operation of the grid-connected energy hubs and the regional renewable power system, the following items were considered as inputs to the optimization problem:

- The required data for modeling thermal units and the regional power system are available in (Alabdulwahab et al. (2017)).

- Bus 1 was considered as the slack bus.

- The minimum required up/down flexible ramping reserves at each scheduling interval were considered to be 35 MW and 30 MW, respectively.

- The cost of up/down flexible ramping reserves for each thermal unit was assumed to be 10% of the first-order coefficient of the fuel cost function (c_i) (Zhang et al. (2016)).

- The installed capacity of the wind farm was equal to 200 MW.

- The cost of wind power curtailment was assumed to be 20 \$/MW and the wholesale natural gas price was set to 15 \$/MWh (Yan et al. (2019)).

- The carbon emission price was set to 20 \$/ton CO_2, and the emission rates of thermal, CHP, and GB units were set to 1.01, 0.386, and 0.204 ton CO_2/MWh, respectively (Yi et al. (2018)).
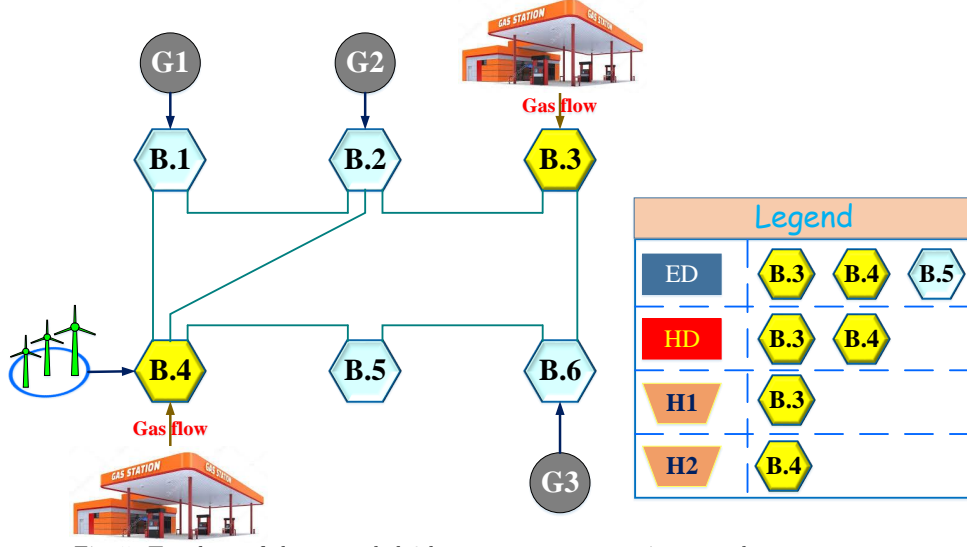

Fig. 5: Topology of the upgraded 6-bus test system as an integrated energy system.

Two energy hub systems were embedded in buses 3 and 4, which are labeled as H1 and H2, respectively. The different modes of allocating energy storage systems and energy conversion facilities to each energy hub system in different case studies were as follows:

In case 1, H1 was equipped with only one CHP unit. On the other hand, H2 was equipped with one CHP unit and one GB unit.

In cases 2 and 3, H1 was equipped with one CHP unit, one EES system, and one TES system. In addition, H2 was equipped with one CHP unit, one GB unit, one P2H storage, and one EES system.

The essential parameters for each element of the energy hub system are given in Table 3 (Mirzaei et al. (2020)). The hourly power and heat demands, and also the forecasted wind power for 24-hour are shown in Fig. 6. Electrical loads connected to the buses 3, 4, and 5 had 20%, 40%, and 40% share of the total demand, respectively. Moreover, heat loads connected to the buses 3 and 4 had 45% and 55% share of the total demand, respectively.

Table 3: Specifications of the available equipment in energy hub systems (Mirzaei et al. (2020)).

Parameter	Amount	Parameter	Amount
η_q, η_g	0.35, 0.8	$\overline{P_{ph}}$ (MW)	20
$\eta_{(.)}^{ch}, \eta_{(.)}^{dis}$	0.9, 0.9	$\underline{S_{ph}}, \overline{S_{ph}}$ (MWh)	0, 60
$\underline{P_q}, \overline{P_q}$ (MW)	45, 160	$\overline{P_{es}^{ch}}, \overline{P_{es}^{dis}}$ (MW)	15, 15
$\underline{H_q}, \overline{H_q}$ (MW)	0, 115	$\underline{S_{es}}, \overline{S_{es}}$ (MWh)	10, 70
$\underline{H_g}, \overline{H_g}$ (MW)	0, 35	$\overline{H_{ts}^{ch}}, \overline{H_{ts}^{dis}}$ (MW)	15, 15
$\underline{\beta_{loss}}, \underline{\beta_{gain}}$	0.3, 0.6	$\underline{S_{ts}}, \overline{S_{ts}}$ (MWh)	0, 60
$\overline{H_{ph}^{ch}}, \overline{H_{ph}^{dis}}$ (MW)	20, 20	cop_{ph}	1.5

5.1.1. Energy dispatch results and technical comparison

The optimal hourly scheduling of thermal units G1, G2, and G3 in various case studies are presented in Figs. 7-9. As it is shown, unit G1 acted as the main source to cover the demands of electricity at each scheduling interval, which is due to the lower operating costs of this unit compared to other thermal

units. In addition, units G2 and G3, as the most expensive units, were operated in a limited interval to meet the remaining demands and to satisfy the technical constraints. For instance, in case 1, unit G2 was turned on from 11 to 15 for five hours. So, units G2 and G3 were utilized when either the electrical load was higher especially in peak intervals or the production level of the wind farm was lower. Furthermore, it can be found that the thermal units provide approximately 54% of the required total electrical demand in each case study. The remaining fractions of electric demand were provided by the wind farm, energy hub systems, and the impressive capabilities of DRPs.

The amount of electricity, gas, and heat exchanged between the energy hub systems and the integrated energy system are shown in Figs. 10-12 for each case study. The positive amounts correspond to imports of power and gas from the upstream energy networks into the energy hub systems and negative amounts demonstrate the power and heat exports from energy hub systems into the district energy networks in the context of the integrated energy system. According to these figures, in cases 2 and 3, the imported natural gas was decreased by about 571 MW (about 10.5%) and 3021 MW (about 55%), respectively, compared to case 1. In all case studies, the injected natural gas is delivered to the CHP and GB units to cover the heat and/or electricity demands. Due to the implementation of multi-energy DRP, the lowest amount of the generated electrical power and heat belonged to case 3. For instance, the exported power at all scheduling periods was decreased by up to 55% in case 3 with respect to case 1. Thus, it can be seen that the optimal dispatch of energy hub systems with multiple input/output ports in coordinated action with technical tools play an undeniable role in increasing the flexibility of the integrated energy system by fully exploiting the available opportunities in each energy market.

In cases 2 and 3, the injected electrical power into the energy hub systems was used to activate the energy storage systems and P2H storage. According to Figs. 11 and 12, in case 3, the total imported powers from the regional power system to the energy hub systems were increased by about 40% compared to case 2. On the other hand, EESs had similar performance in cases 2 and 3 by storing 154 MW in charging mode. Therefore, the difference in the amount of imported power into the energy hub systems in cases 2 and 3 was directly related to the performance of the P2H storage. The hourly scheduling of P2H storage in cases 2 and 3 are shown in Figs. 13 and 14. As can be seen from these figures, the total
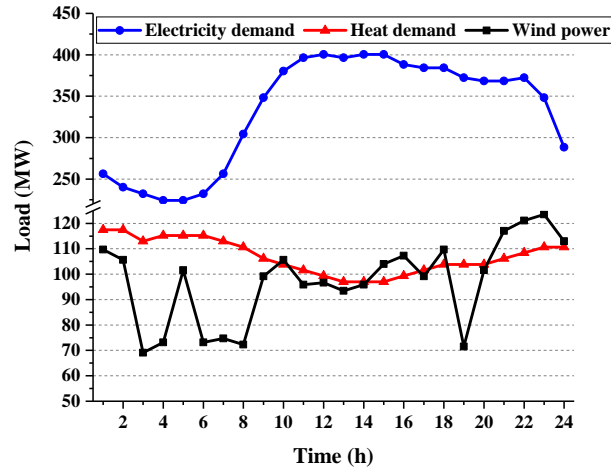

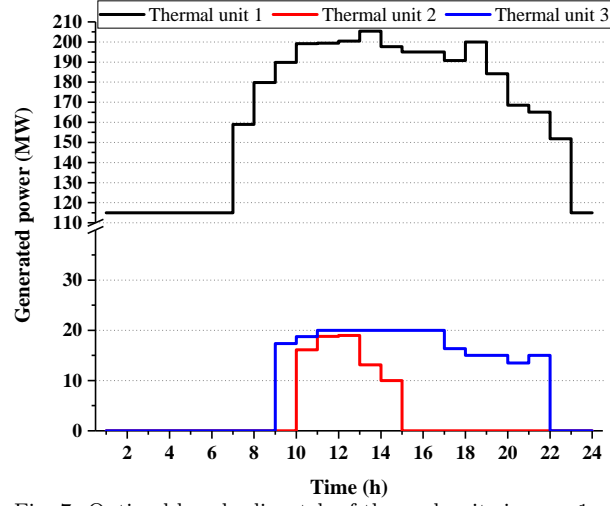Fig. 6: Electrical demand, heat demand, and wind power of 6-bus system.

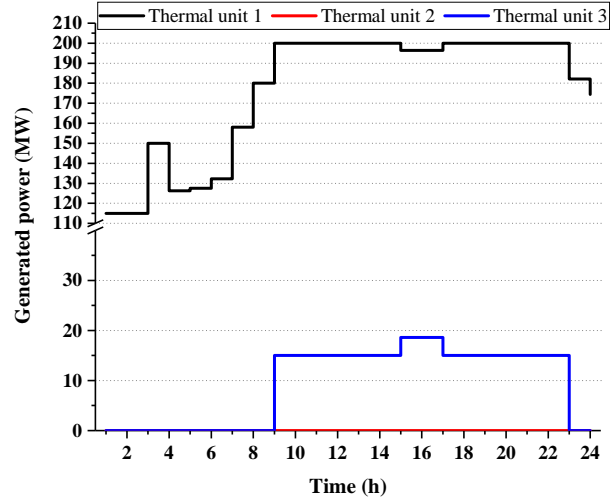Fig. 7: Optimal hourly dispatch of thermal units in case 1.

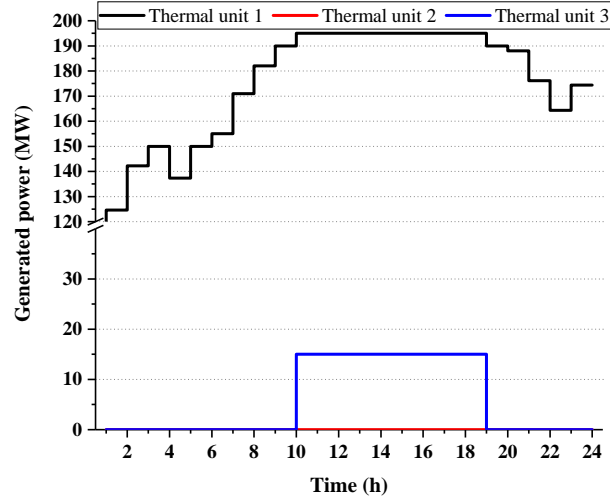Fig. 8: Optimal hourly dispatch of thermal units in case 2.

Fig. 9: Optimal hourly dispatch of thermal units in case 3.

heat production by P2H storage was increased by 270 MW (i.e., 65%) in case 3 compared to case 2. In times when the wind farm produced more than the capacity of the regional power system lines, the system operator converted the extra generated wind power into heat by P2H technology. The produced heat can
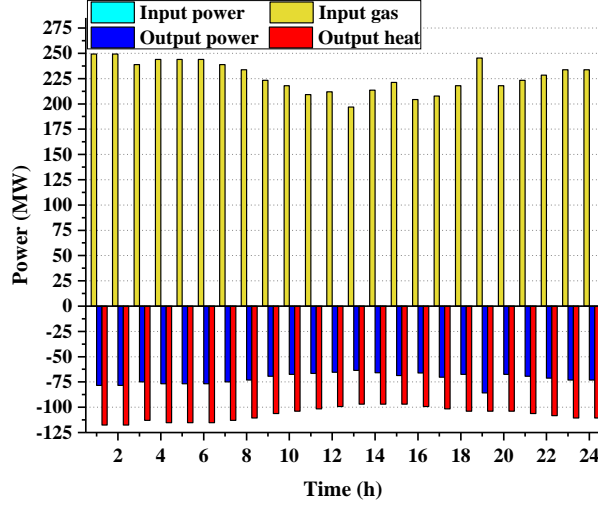
Fig. 10: Optimal hourly scheduling of energy hub systems in case 1.
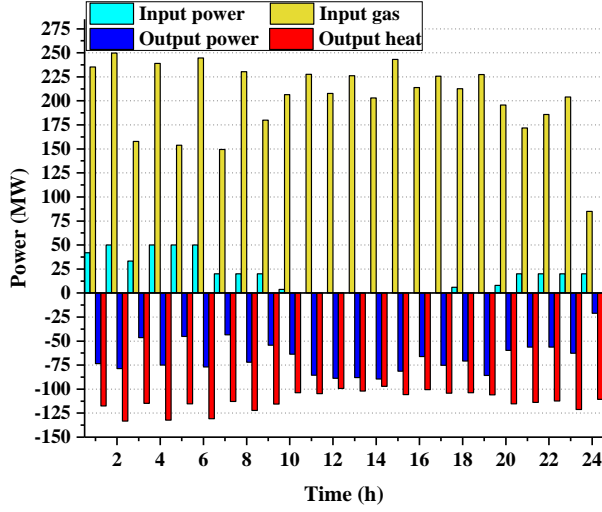
Fig. 11: Optimal hourly scheduling of energy hub systems in case 2.
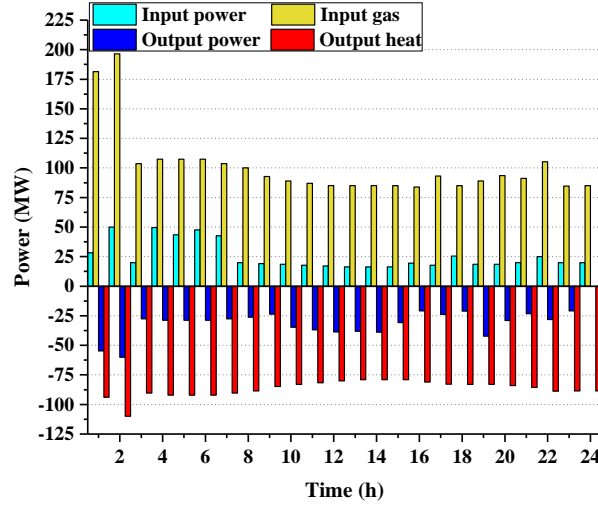
Fig. 12: Optimal hourly scheduling of energy hub systems in case 3.

be stored in the storage systems or delivered directly to the existing district heat networks to meet heat demands. According to Figs. 13 and 14, it can be seen that the P2H storage was heavily used at all scheduling intervals to make optimal decisions to save the total operating cost of the integrated system,

reduce wind power curtailment, and decrease CO_2 emission cost.
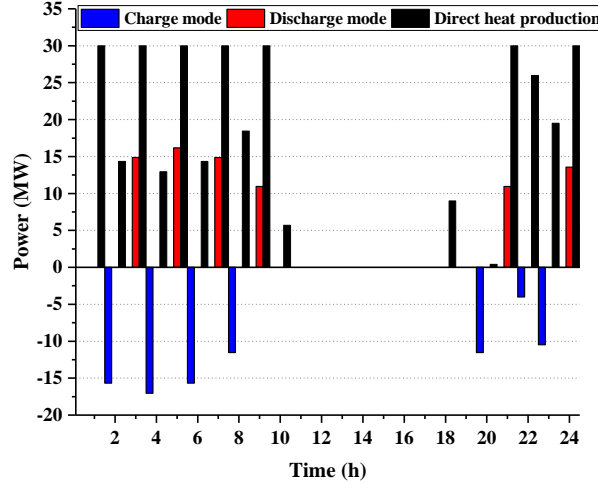
Fig. 13: Optimal hourly scheduling of P2H storage in case 2.
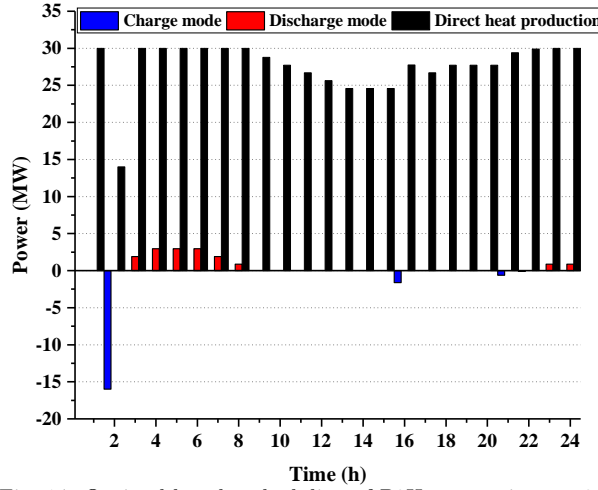
Fig. 14: Optimal hourly scheduling of P2H storage in case 3.

In the third case study, the impacts of multi-energy DRP in coordination with other flexible resources (i.e., EES, TES, and P2H storage) were considered in integrated energy system operation simultaneously. In this study, the multi-energy DRP was implemented based on the incentive-based procedure, which was handled by the load curtailment option. Hence, the incentive values were assumed to be 30 \$/MWh and 20 \$/MWh for the electrical and heat loads, respectively. Furthermore, the participation rates of electrical and heat loads for implementing multi-energy DRP were set to be 30% and 20%, respectively. Figs. 15 and 16 demonstrate the consequence of multi-energy DRP on the electrical and heat load profiles of the integrated energy system. By implementing the multi-energy DRP, the system operator can use the unique capability of this technique to reduce the total operating costs and wind power curtailment. The total electrical and heat loads of the regional energy system were reduced by up to 14.8% and 20%, respectively, which can be one of the reasons for improving the performance of the regional energy system from the technical and economic point of view.

The total amount of wind power curtailment for each case study with regards to the defined actions is shown in Fig. 17. In case 1, the amount of curtailed wind power was equal to 12.67% of the total forecasted
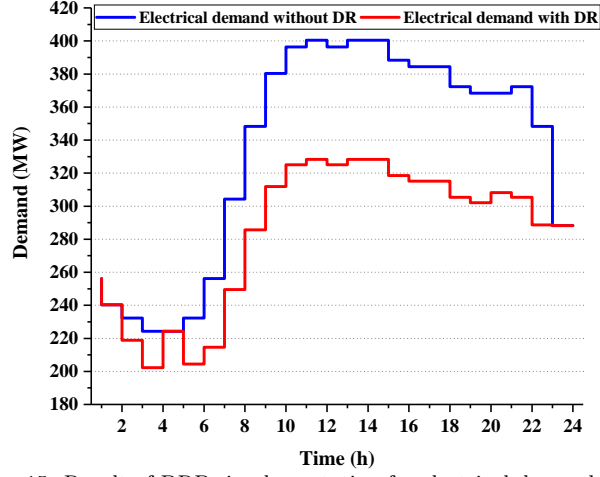
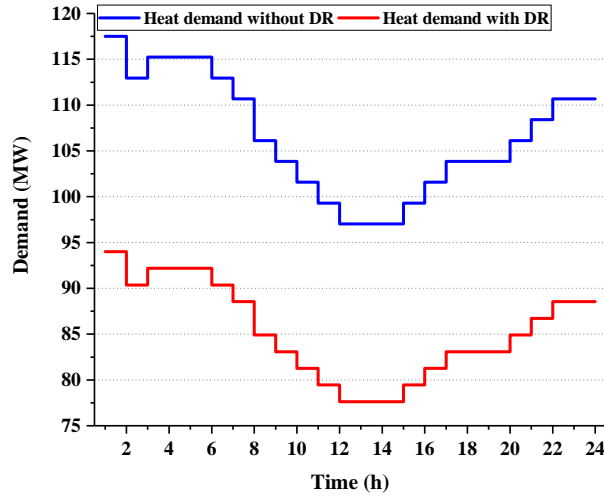Fig. 15: Result of DRPs implementation for electrical demands.

Fig. 16: Result of DRPs implementation for heat demands.

wind power. In case 2, the amount of curtailed power was significantly reduced in comparison with the case 1 using P2H storage, EESs, and TESs. As shown in Fig. 17, the total wind power curtailment only occurred in one interval (at 02:00 o'clock) and the spilled power amount was equal to 9 MW. Finally, with the simultaneous use of the multi-energy DRP and energy storage systems in the framework of the energy hub systems, the amount of curtailed wind power had reached zero.

In order to investigate the regional power system from the perspective of the congestion issue, the amount of power flow between the system lines should be calculated using (51) during each scheduling period. The loading limit margin in system lines was assumed to be 80% of the maximum loading capacity for each line. Fig. 18 shows the total number of transmission lines in which the power flow rate was exceeded the allowable range during the entire scheduling horizon (24 hours). In cases 2 and 3, the congestion was relieved by applying the presented approaches. Energy conversion technologies in the form of energy hub systems were playing a significant role in relieving congestion by providing the required electrical demand using the natural gas source.
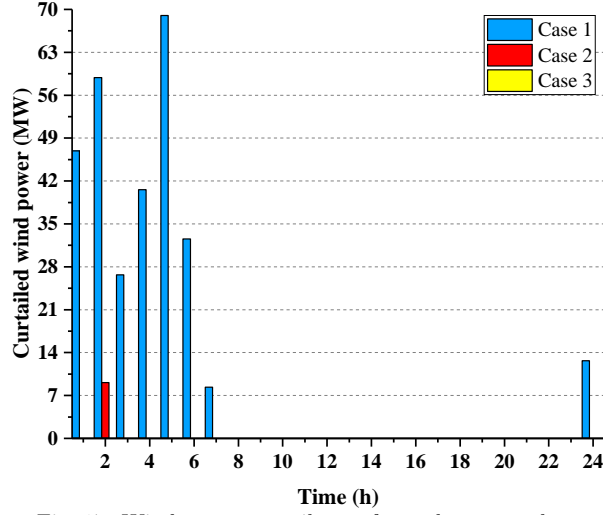
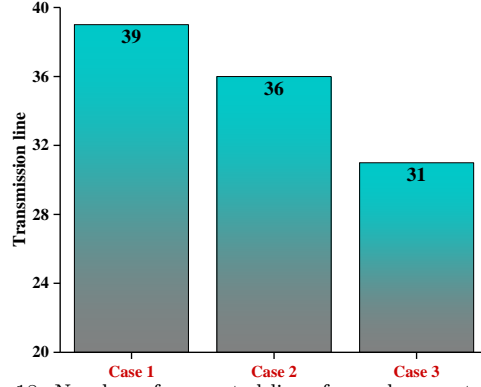Fig. 17: Wind power curtailment for each case study.

Fig. 18: Number of congested lines for each case study.

5.1.2. Economic comparison

A comprehensive economic analysis of the integrated energy system performance is given in Table 4. The results demonstrate that the cost of CO_2 emission and wind power curtailment, as well as the total operating cost of the integrated energy system, can be reduced by adopting the optimal coordinated strategy between the regional power system and grid-connected energy hub systems. According to this table, the P2H storage was able to significantly decrease the cost of wind power curtailment caused by both line flow limits and power balance constraint. Furthermore, case 3 (with multi-energy DRP implementation) had a significantly lower total operating cost in comparison with cases 1 and 2 (without multi-energy DRP implementation). An improvement of 16.62% in the total operating cost compared to case 1 indicated the tremendous economic impact of the multi-energy DRP implementation.

The use of the grid-connected energy hubs in coordination with the regional power system can also modify LMPs. The average LMPs of the 6-bus test system buses for each case study are shown in Fig. 19. According to the figure, utilization of the P2H storages and multi-energy DRP had a significant impact on the LMPs. The average LMPs in cases 2 and 3 were reduced during periods 10-20 compared to case 1. For example, the average LMPs at hour 15 was decreased from 65.52 $/MWh in case 1 to 52.84 $/MWh in case 3. The 12.68 $/MWh drop was due to the selection of the marginal thermal unit. As shown in Fig. 9, the expensive thermal unit G2 was not committed at hour 15 in case 3. On the contrary, the average

Table 4: Economical comparison of case studies in the 6-bus test system.

	Case 1	Case 2	Case 3
CO_2 emissions cost (\$)	164,565.21	153,956.12	114,455.12
Operating cost of thermal units (\$)	66,277.52	67,806.17	64,514.48
Cost of flexible ramping reserve (\$)	12,984.86	14,170.77	15,382.46
Operating cost of energy hub systems (\$)	81,728.01	73,155.67	36,408.20
Incentive compensation costs of multi-energy DRP (\$)	0	0	45,612.59
Cost of wind power curtailment (\$)	5,912.21	181.79	0
Total operating cost (\$)	**331,467.81**	**309,270.52**	**276,372.85**
Operating cost decrement (%)	**-**	**6.7**	**16.62**

LMPs were increased at the initial intervals of the scheduling program in cases 2 and 3 compared to case 1. The reason for this was that the energy storage systems were charged in these intervals. On the other hand, because the number of congested lines in cases 2 and 3 were less than case 1, the average LMPs in cases 2 and 3 were also less than case 1. This fact was previously shown in Fig. 18.
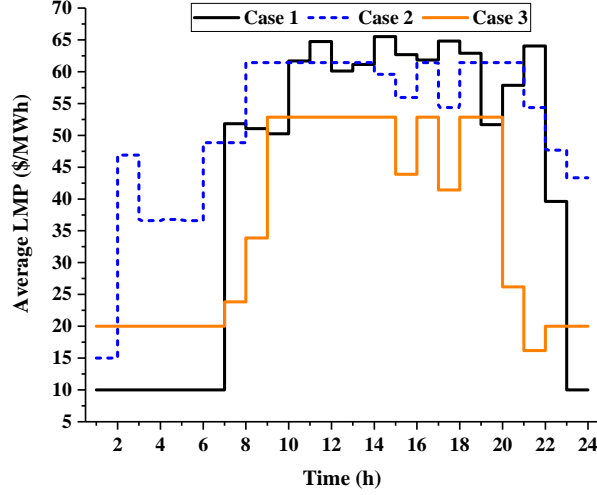

Fig. 19: The impact of using energy hubs on LMPs of the 6-bus test system.

5.1.3. Effects of the wind power uncertainty on the scheduling process

In case 4, the uncertainty posed by wind power was considered using the IGDT-based robust SCUC model. Based on the explanations provided in sub-section 3.8, the base value of operating cost (TC_d) was considered as the obtained amount in case 1, i.e., \$331,467.81. In addition, the rate of cost deviation factor (β_r) was considered from 0 to 0.1 with ten equal intervals (0, 0.01, 0.02,...). The variations of the optimum robustness function ($\tilde{\alpha}$) with regards to β_r for cases 1 and 3 are illustrated in Fig. 20. It is clear that the impact of β_r coefficient changes on critical operation cost and $\tilde{\alpha}$ is extremely high. For example, for $\beta_r = 0.05$, the critical operating cost was guaranteed at least \$348,041.22 while the wind power variations compared to the forecasted value were more than 25%. As well, the optimum robustness function in case 3 had high value compared to case 1. The simulation results indicated that increasing β_r coefficient can help to boost the optimal robustness function in both case studies.
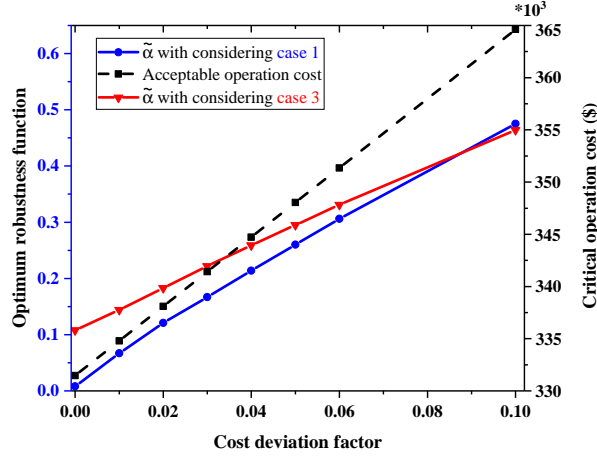
Fig. 20: Optimum robustness function with regard to deviation factor.

5.2. Modified 24-bus test system

To evaluate the presented IGDT-based robust SCUC model in a large-scale power system, the modified 24-bus test system was considered with ten thermal units, two wind farms as the uncertain sources, four energy hub systems, seventeen electrical loads, and four heat loads. The schematic diagram of the network is shown in Fig. 21. To use the proposed model, the following items were considered as inputs to the optimization problem:

- All technical data related to the regional power system can be obtained from (Grigg et al. (1999)).
- Bus 13 was considered as the slack bus.
- The maximum power capacity of each wind farm was considered to be 350 MW and these units were installed on buses 4 and 6.
- The forecasted wind power profiles for each wind farm follow the used pattern in the 6-bus test system.

The energy hub systems were installed on buses 4, 6, 8, and 17, which are labeled as H1 to H4. The various energy conversion facilities that were used in each energy hub system to perform different case studies are as follows:

In case 1, H1 and H3 were equipped with one CHP unit and one GB unit. On the other hand, H2 and H4 were equipped with only one CHP unit.

In cases 2 and 3, H1 was equipped with one CHP unit and one GB unit. H2 was equipped with one CHP unit, one P2H storage, and one TES system. H3 was equipped with one CHP unit, one GB unit, one TES system, and one EES system. In addition, H4 was equipped with one CHP unit, one P2H storage, and one EES system.

The technical specifications of the available equipment in energy hub systems were considered to be similar to the 6-bus test system as shown in Table 3. The hourly power and heat load curves are shown in Fig. 22. In addition, the total electrical and heat loads were distributed and allocated in different buses according to Table 5.
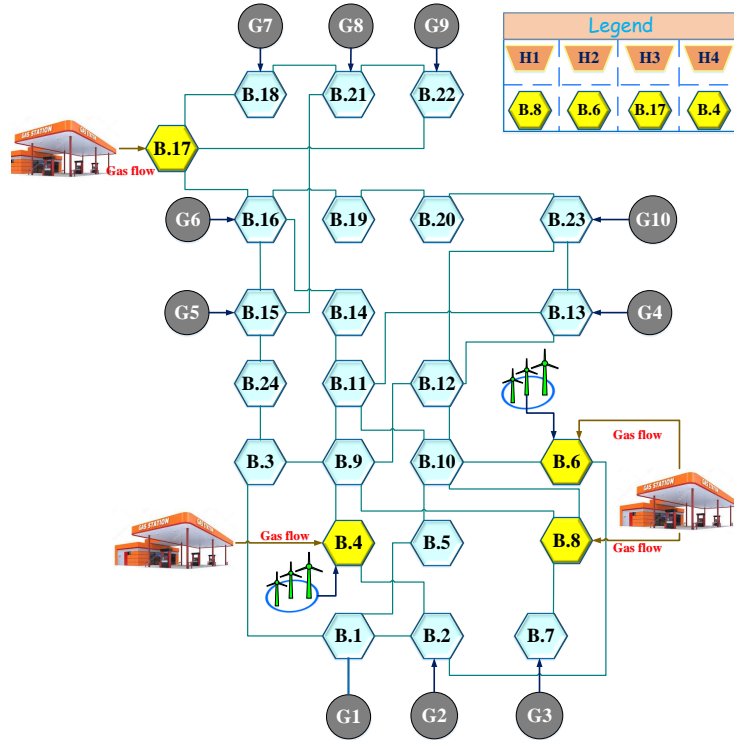
Fig. 21: Topology of the upgraded 24-bus test system as an integrated energy system.
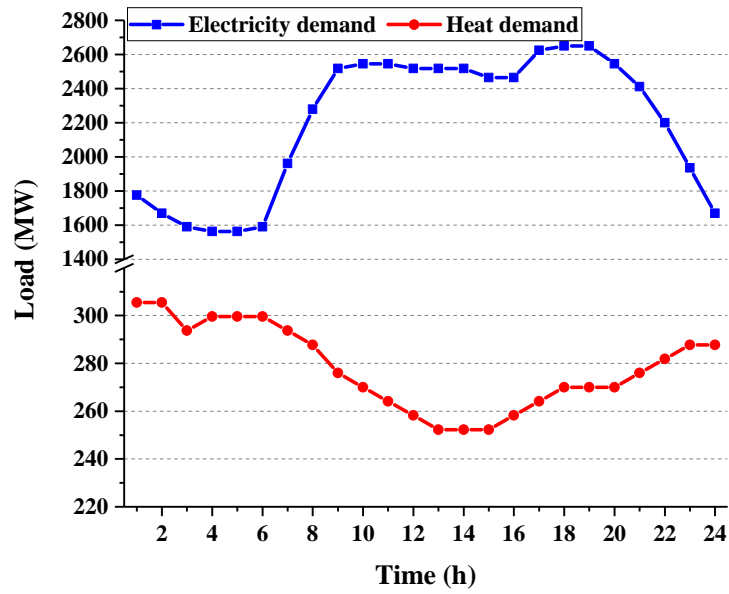

Fig. 22: Total electrical and heat loads of 24-bus system.

Table 5: Electrical and heat loads location and distribution.

Electrical load	Bus	Distribution coefficient (%)	Electrical load	Bus	Distribution coefficient (%)	Heat load	Bus	Distribution coefficient (%)
1	1	3.8	10	10	6.8	1	8	25
2	2	3.4	11	13	9.3	2	6	28
3	3	6.3	12	14	6.8	3	17	15
4	4	2.6	13	15	11.1	4	4	32
5	5	2.5	14	16	3.5			
6	6	4.8	15	18	11.7			
7	7	4.4	16	19	6.4			
8	8	6	17	20	4.5			
9	9	6.1						

All case studies previously defined for the modified 6-bus test system were also included in this test system. Fig. 23 shows the wind power curtailment for each case study in the framework of the modified 24-bus test system. As can be seen in this figure, in comparison with case 1, the rate of wind power curtailment was decreased significantly in other case studies. So that the amount of wind power curtailment in case 3 was almost zero. Therefore, the energy hub systems, which were equipped with up-to-date facilities, in coordination with multi-energy DRP can be considered as the best approach to reduce renewable power curtailment. Furthermore, the economic impacts of the use of promoted energy hub systems as well as multi-energy DRP on the total operating cost of the integrated energy system are given in Table 6. In case 1, the costs of CO_2 emission and wind power curtailment were very high compared to other cases, so the operating cost of the integrated energy system had the highest amount in this case study.
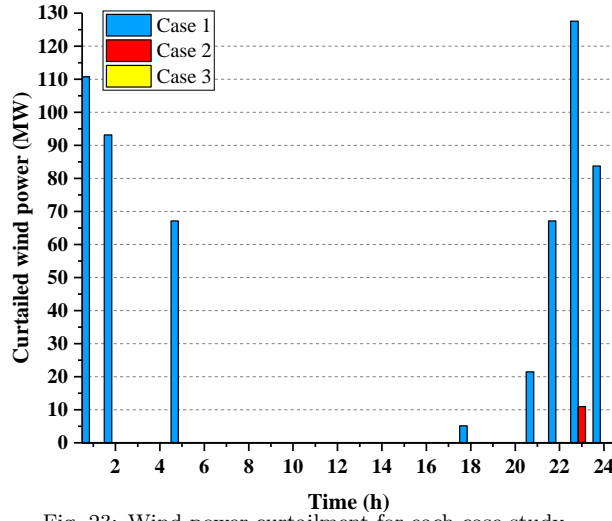

Fig. 23: Wind power curtailment for each case study.

Table 6: Economical comparison of case studies in the 24-bus test system.

	Case 1	Case 2	Case 3
CO_2 emissions cost (\$)	977,345.97	949,479.22	642,886.39
Operating cost of thermal units (\$)	428,866.05	455,418.84	287,034.32
Cost of flexible ramping reserve (\$)	4,447.79	5,577.13	5,243.77
Operating cost of energy hub systems (\$)	261,333.97	169,809.62	139,396.57
Incentive compensation costs of multi-energy DRP (\$)	0	0	438,989.98
Cost of wind power curtailment (\$)	11,522.41	219.02	0.37
Total operating cost (\$)	**1,683,516.19**	**1,580,503.83**	**1,513,551.40**
Operating cost decrement (%)	**-**	**6.12**	**10.09**

The impact of coordinated scheduling of the regional power system and grid-connected energy hubs on the average LMPs is also shown in Fig. 24. According to this figure, although by utilizing P2H in case 2, the average LMPs were increased during periods 5-14, these amounts were decreased significantly during periods 16-24. Likewise, utilization of the multi-energy DRP in case 3 reduced the LMPs during the hours between 8 and 24.

In order to ensure optimum and sustainable exploitation of the integrated energy system under wind
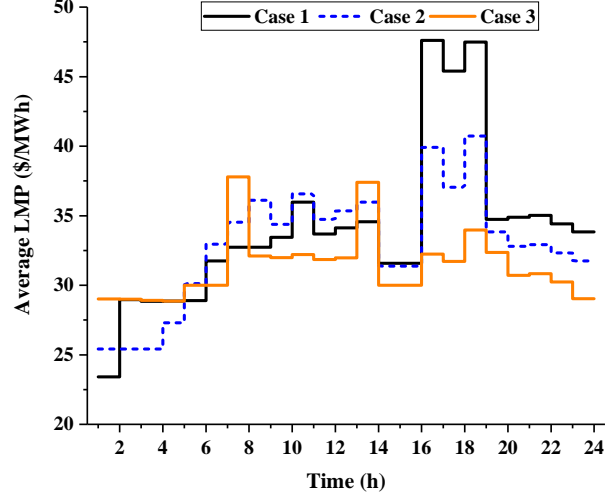
Fig. 24: The impact of using energy hubs on LMPs of the 24-bus test system.

power uncertainty, the proposed IGDT-based robust SCUC model was used to determine the optimum operational strategy. The base level of the operating cost was assumed to be \$1,683,516.19 and the rate of β_r was considered in the range of 0 to 0.1. The optimum robustness functions and critical operation costs, according to the different values of β_r parameter are illustrated in Fig. 25. Therefore, it can be concluded that the flexibilities of the promoted energy hub systems and multi-energy DRP were effective to compensate for the uncertainty in wind farms generation.
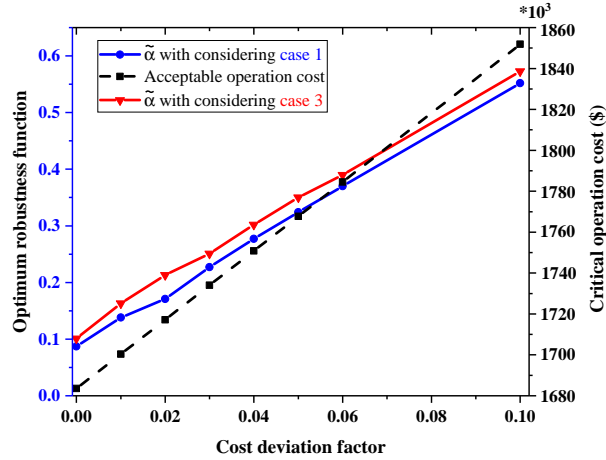

Fig. 25: Optimum robustness function with regard to deviation factor.

6. Conclusions and future work

This paper proposed a developed IGDT-based robust scheduling strategy for optimal coordination of the grid-connected energy hubs with the regional power grid in the framework of the integrated energy systems under high penetration of wind power generation. The main focus of this article was to design and implement a holistic day-ahead scheduling program to simultaneously minimize integrated energy system operational costs, wind power curtailment, and carbon emissions. In addition, the participation of multi-energy consumers in integrated energy system management was investigated through the concept of multi-energy DRP to enhance the effectiveness of the proposed strategy in decreasing operational

31

costs. Two well-known standard test systems were considered to analyze the performance of the proposed strategy. The robustness of the proposed strategy was tested through several case studies. Simulation results indicated that the coordinated operation of the regional power system and promoted energy hub systems using the proposed strategy was very effective in increasing the degree of freedom in decision-making as well as achieving the intended goals. Numerical results in the 6-bus test system showed that using up-to-date energy conversion facilities such as P2H storage can reduce the total operation cost by up to 6.7%. The results also showed that the total operation cost could be further decreased by up to 16.62% by implementing multi-energy DRP. From an environmental point of view, the technical results show that the use of the P2H storage in coordination with multi-energy DRP was provided the required conditions for 100% utilization of the installed wind farms. Further, the CO_2 emissions cost was \$114,455.12 in case 3 that was the lowest amount of case studies and was about 69.9% of its corresponding amount of the first case study. Meanwhile, the impact of the wind power uncertainty on the results was analyzed through the IGDT-based robust approach.

In the future work, a comprehensive optimization program for integrating the regional and district energy systems will be used to more accurately examine the performance of the regional power system as well as other important entities in the context of the multi-carrier energy system.

Acknowledgment

References

Abdollahi, E., & Lahdelma, R. (2020). Decomposition method for optimizing long-term multi-area energy production with heat and power storages. *Applied Energy*, *260*, 114332.

Alabdulwahab, A., Abusorrah, A., Zhang, X., & Shahidehpour, M. (2017). Stochastic security-constrained scheduling of coordinated electricity and natural gas infrastructures. *IEEE Systems Journal*, *11*, 1674–1683.

Behboodi, S., Chassin, D. P., Djilali, N., & Crawford, C. (2017). Interconnection-wide hour-ahead scheduling in the presence of intermittent renewables and demand response: A surplus maximizing approach. *Applied Energy*, *189*, 336 – 351.

Chen, K., Wu, W., Zhang, B., & Sun, H. (2015a). Robust restoration decision-making model for distribution networks based on information gap decision theory. *IEEE Transactions on Smart Grid*, *6*, 587–597.

Chen, X., Kang, C., O'Malley, M., Xia, Q., Bai, J., Liu, C., Sun, R., Wang, W., & Li, H. (2015b). Increasing the flexibility of combined heat and power for wind power integration in china: Modeling and implications. *IEEE Transactions on Power Systems*, *30*, 1848–1857.

Chen, X., Lv, J., McElroy, M. B., Han, X., Nielsen, C. P., & Wen, J. (2018). Power system capacity expansion under higher penetration of renewables considering flexibility constraints and low carbon policies. *IEEE Transactions on Power Systems*, *33*, 6240 – 6253.

Davatgaran, V., Saniei, M., & Mortazavi, S. S. (2019). Smart distribution system management considering electrical and thermal demand response of energy hubs. *Energy*, *169*, 38 – 49.

Deng, X., & Lv, T. (2020). Power system planning with increasing variable renewable energy: A review of optimization models. *Journal of Cleaner Production*, *246*, 118962.

Dini, A., Pirouzi, S., Norouzi, M., & Lehtonen, M. (2019). Grid-connected energy hubs in the coordinated multi-energy management based on day-ahead market framework. *Energy*, *188*, 116055.

Dui, X., Zhu, G., & Yao, L. (2018). Two-stage optimization of battery energy storage capacity to decrease wind power curtailment in grid-connected wind farms. *IEEE Transactions on Power Systems*, *33*, 3296 – 3305.

Eladl, A. A., El-Afifi, M. I., Saeed, M. A., & El-Saadawi, M. M. (2020). Optimal operation of energy hubs integrated with renewable energy sources and storage devices considering CO_2 emissions. *International Journal of Electrical Power & Energy Systems*, *117*, 105719.

Grigg, C., Wong, P., Albrecht, P., Allan, R., Bhavaraju, M., Billinton, R., Chen, Q., Fong, C., Haddad, S., Kuruganty, S., Li, W., Mukerji, R., Patton, D., Rau, N., Reppen, D., Schneider, A., Shahidehpour, M., & Singh, C. (1999). The ieee reliability test system-1996. a report prepared by the reliability test system task force of the application of probability methods subcommittee. *IEEE Transactions on Power Systems*, *14*, 1010–1020.

Khaloie, H., Abdollahi, A., Shafie-Khah, M., Siano, P., Nojavan, S., Anvari-Moghaddam, A., & Catalão, J. P. (2020). Co-optimized bidding strategy of an integrated wind-thermal-photovoltaic system in deregulated electricity market under uncertainties. *Journal of Cleaner Production*, *242*, 118434.

Kong, L., Li, Z., Liang, L., Xia, Y., & Xie, J. (2018). A capacity-investment model of wind power with uncertain supply-price under high penetration rate. *Journal of Cleaner Production*, *178*, 917 – 926.

Li, Y., Li, Z., Wen, F., & Shahidehpour, M. (2019). Privacy-preserving optimal dispatch for an integrated power distribution and natural gas system in networked energy hubs. *IEEE Transactions on Sustainable Energy*, *10*, 2028–2038.

Li, Y., Wang, J., Han, Y., Zhao, Q., Fang, X., & Cao, Z. (2020). Robust and opportunistic scheduling of district integrated natural gas and power system with high wind power penetration considering demand flexibility and compressed air energy storage. *Journal of Cleaner Production*, *256*, 120456.

Liang, J., & Tang, W. (2020). Interval based transmission contingency-constrained unit commitment for integrated energy systems with high renewable penetration. *International Journal of Electrical Power & Energy Systems*, *119*, 105853.

Majidi, M., Mohammadi-Ivatloo, B., & Soroudi, A. (2019). Application of information gap decision theory in practical energy problems: A comprehensive review. *Applied Energy*, *249*, 157 – 165.

Mirzaei, M. A., Oskouei, M. Z., Mohammadi-Ivatloo, B., , Loni, A., Zare, K., Marzband, M., & Shafiee, M. (2020). Integrated energy hub system based on power-to-gas and compressed air energy storage technologies in the presence of multiple shiftable loads. *IET Generation, Transmission & Distribution*, *14*, 2510–2519(9).

Mirzaei, M. A., Sadeghi-Yazdankhah, A., Mohammadi-Ivatloo, B., Marzband, M., Shafie-khah, M., & Catalão, J. P. (2019). Integration of emerging resources in igdt-based robust scheduling of combined power and natural gas systems considering flexible ramping products. *Energy*, *189*, 116195.

Mohammadi, M., Noorollahi, Y., Mohammadi-ivatloo, B., & Yousefi, H. (2017). Energy hub: From a model to a concept – a review. *Renewable and Sustainable Energy Reviews*, *80*, 1512 – 1527.

Mohammadi-Ivatloo, B., Zareipour, H., Amjady, N., & Ehsan, M. (2013). Application of information-gap decision theory to risk-constrained self-scheduling of gencos. *IEEE Transactions on Power Systems*, *28*, 1093–1102.

Oskouei, M. Z., & Yazdankhah, A. S. (2015). Scenario-based stochastic optimal operation of wind, photovoltaic, pump-storage hybrid system in frequency- based pricing. *Energy Conversion and Management*, *105*, 1105 – 1114.

Oskouei, M. Z., & Yazdankhah, A. S. (2017). The role of coordinated load shifting and frequency-based pricing strategies in maximizing hybrid system profit. *Energy*, *135*, 370 – 381.

Soroudi, A., Rabiee, A., & Keane, A. (2017). Information gap decision theory approach to deal with wind power uncertainty in unit commitment. *Electric Power Systems Research*, *145*, 137 – 148.

GWEC (2019). Global wind energy council (GWEC), [online]. available at: https://gwec.net/global-wind-report-2019/, .

IEA (2019). International energy agency (IEA), [online]. available at: https://www.iea.org/reports/world-energy-outlook-2019, .

Wang, B., Zhou, M., Xin, B., Zhao, X., & Watada, J. (2019a). Analysis of operation cost and wind curtailment using multi-objective unit commitment with battery energy storage. *Energy*, *178*, 101 – 114.

Wang, D., Qiu, J., Reedman, L., Meng, K., & Lai, L. L. (2018). Two-stage energy management for networked microgrids with high renewable penetration. *Applied Energy*, *226*, 39 – 48.

Wang, J., Hu, Z., & Xie, S. (2019b). Expansion planning model of multi-energy system with the integration of active distribution network. *Applied Energy*, *253*, 113517.

Xie, S., Hu, Z., & Wang, J. (2020a). Two-stage robust optimization for expansion planning of active distribution systems coupled with urban transportation networks. *Applied Energy*, *261*, 114412.

Xie, S., Hu, Z., Wang, J., & Chen, Y. (2020b). The optimal planning of smart multi-energy systems incorporating transportation, natural gas and active distribution networks. *Applied Energy*, *269*, 115006.

Xie, S., Hu, Z., Zhou, D., Li, Y., Kong, S., Lin, W., & Zheng, Y. (2018). Multi-objective active distribution networks expansion planning by scenario-based stochastic programming considering uncertain and random weight of network. *Applied Energy*, *219*, 207 – 225.

Yan, M., Zhang, N., Ai, X., Shahidehpour, M., Kang, C., & Wen, J. (2019). Robust two-stage regional-district scheduling of multi-carrier energy systems with a large penetration of wind power. *IEEE Transactions on Sustainable Energy*, *10*, 1227–1239.

Yi, J. H., Ko, W., Park, J.-K., & Park, H. (2018). Impact of carbon emission constraint on design of small scale multi-energy system. *Energy*, *161*, 792 – 808.

Zhang, X., Che, L., Shahidehpour, M., Alabdulwahab, A., & Abusorrah, A. (2016). Electricity-natural gas operation planning with hourly demand response for deployment of flexible ramp. *IEEE Transactions on Sustainable Energy*, *7*, 996–1004.